Organic & Biomolecular Chemistry

PAPER

View Article Online
View Journal | View Issue

Cite this: *Org. Biomol. Chem.*, 2015, **13**, 3803

Design, synthesis and biological evaluation of 1-phenanthryl-tetrahydroisoquinoline derivatives as novel p21-activated kinase 4 (PAK4) inhibitors†

Shuai Song,‡[a] Xiaodong Li,‡[b] Jing Guo,[a] Chenzhou Hao,[a] Yan Feng,[a] Bingyu Guo,[b] Tongchao Liu,[a] Qiaoling Zhang,[a] Zhen Zhang,[a] Ruijuan Li,[a] Jian Wang,[a] Bin Lin,[a] Feng Li,*[b] Dongmei Zhao*[a] and Maosheng Cheng*[a]

Received 8th January 2015,
Accepted 9th February 2015

DOI: 10.1039/c5ob00037h

www.rsc.org/obc

Functional versatility and elevated expression in cancers have promoted p21-activated kinase 4 (PAK4) as one of the first-in-class anti-cancer drug targets. In this study, a series of novel 1-phenanthryl-tetrahydroisoquinoline analogues have been designed and synthesized as a novel class of small-molecule PAK4 inhibitors to fit into the cavity of PAK4. All of the target compounds were evaluated for their *in vitro* PAK4 inhibitory activities and antiproliferative activities. Lead optimization identified all the derivatives with more potency than the lead compound, especially compound **21a**. Moreover, compound **21a** significantly induced the cell cycle in the G1/S phase, and inhibited migration and invasion of MCF-7 cells *via* the regulation of the PAK4-LIMK1-cofilin signaling pathway. A molecular modeling study showed possible novel binding modes between **21a** and PAK4 and provided a structural basis for further structure-guided design of PAK4 inhibitors.

Introduction

PAKs (p21-activated kinases) comprise a family of Ser/Thr kinases that are activated by Ras-related G proteins of 21 kDa (p21) called Rac and CDC42.[1,2] In 1977, the first member of the PAK family was isolated at NIH from a soil amoeba as Acanthamoeba myosin I heavy chain kinase (MIHCK).[3] They are thought to play an important role in numerous cancer cellular processes, including cytoskeletal signaling pathways, cell cycle progression, cancer cell invasion and migration, cell survival and apoptosis, and therefore have been extensively studied since their discovery.[4–7]

Six different PAKs have been classified into two groups (PAK1–3 of group I, and PAK4–6 of group II) based on their domain architectures.[8,9] The group I family has already been studied intensively, and the members of the group II PAK family are now emerging as more interesting targets for cancer therapy.[10] PAK4 as the first identified and characterized member of group II PAK, was widely studied with the most cancer-related citations.[11–13] Recently, a paired recombinant protein assay identified LIM kinase 1 (LIMK1) as a substrate for PAK4 *in vitro*[14,15] which solidly confirmed the previous studies on LIMK1, as a substrate of PAK4 kinase, playing an important role in actin filament dynamics of migrating cells.[16–19] PAK4 is tumorigenic *in vitro* and *in vivo*[13,20] and its overexpressed or genetic amplification is found in numerous cancer cell lines and tumours.[21,22] Therefore, PAK4 is considered as an attractive target for anti-cancer drug design.

A number of ATP-competitive PAK inhibitors have been described in detail in patent applications. PF-3758309, disclosed by Pfizer in 2010,[23,24] is a potent, ATP-competitive, pyrrolopyrazole inhibitor of PAK4. This compound progressed into phase I clinical trials in patients with advanced/metastatic solid tumors. Unfortunately, the phase I clinical trial of PF-3758309 was prematurely terminated due to undesirable pharmacokinetic characteristics and a lack of an observed dose–response relationship; subsequent clinical investigation of PF-3758309 has been placed on hold.[25] Using a high throughput screening and validation, researchers at Soongsil University and Korea Research Institute of Chemical Technology identified KY-04031 as a novel p21-activated kinase 4 inhibitor. The crystal structure of PAK4 complexed with the compound illustrated that both indole and indazole of KY-04031 are responsible for PAK4 hinge interaction. Moreover, the triazine molecular core of KY-04031 mimics the

[a]*Key Laboratory of Structure-Based Drug Design & Discovery of Ministry of Education, Shenyang Pharmaceutical University, Shenyang 110016, P. R. China. E-mail: mscheng@263.net, dongmeiz-67@163.com; Fax: +86-24-23995043; Tel: +86-24-23986413*

[b]*Department of Cell Biology, Key Laboratory of Cell Biology, Ministry of Public Health, and Key Laboratory of Medical Cell Biology, Ministry of Education, China Medical University, Shenyang 110001, P. R. China. E-mail: fli@mail.cmu.edu.cn; Fax: +86-24-23261056; Tel: +86-24-23256666*

†Electronic supplementary information (ESI) available: Details of experimental procedure, spectral data of all novel compounds. See DOI: 10.1039/c5ob00037h

‡These authors contributed equally to this work.

ribose of ATP, distinguishing its unique scaffold from other known PAK4 inhibitors.[26] Researchers from Genentech recently succeeded in identifying a highly potent and highly selective group II PAK-selective inhibitor, with a novel binding mode and exquisite kinome selectivity. Hydrophobic interactions within a lipophilic pocket past the methionine gatekeeper of group II PAKs approached by these type I 1/2 binders were found to be important for improving potency. A concentration-dependent decrease in tumor cell migration and invasion in two triple-negative breast cancer cell lines was observed with this compound.[27]

Herein we describe the identification of novel PAK4 inhibitors with the scaffold of 1-phenanthryl-tetrahydroisoquinoline. The lead compounds from which these compounds are derived were (−)-β-hydrastine (**1**, Fig. 1) and noscapine (**2**, Fig. 1), identified from our in-house natural product database, with moderate inhibition in a PAK4 biochemical assay (IC_{50} = 29.8 μM, 28.5 μM) (manuscript submitted to Expert Opinion on Therapeutic Targets). (−)-β-Hydrastine, comprised of tetrahydroisoquinoline and isobenzofuranone fragments, is a natural product that was first extracted from the root of *Hydrastis canadensis* in 1862 and used as a uterine hemostatic agent, antibacterial agent, and anti-inflammatory agent.[28,29] Recently, (−)-β-hydrastine and noscapine were shown to be microtubule-targeting molecules, then the two agents were evaluated for activity in cell migration and invasion.[30] Because the PAK4 has been linked with survival, proliferation, migration, invasion, and apoptosis in tumors, our group and collaborator Prof. Li from China Medical University first demonstrated that these two natural products mediated their effects by modulating the PAK4 activation pathway in MCF-7 cells (manuscript submitted to Expert Opinion on Therapeutic Targets). However, these compounds contain lactone in their structures therefore are prone to hydrolysis. Our goals for lead optimization were to avoid the stability problems from the isobenzofuranone fragment and simplify the two chiral centers, hoping to maintain the inhibition activity toward PAK4. Different replacements for the isobenzofuranone fragment have been designed, synthesized, and evaluated for their biological activities toward PAK4. Phenanthryl ring as a replacement to afford 1-phenanthryl-tetrahydroisoquinoline derivatives was found to result in the best PAK4 inhibitions. Followed by lead optimization, a novel class of PAK4 inhibitors with the 1-phenanthryl-tetrahydroisoquinoline scaffold was identified. Among them, **21a** was discovered as a unique small-molecule inhibitor of the PAK4 interaction with good affinity (IC_{50} = 8.84 μM). Here, we reported the synthesis, biological evaluation and the structure–activity relationships (SARs) of this series of 1-phenanthryl-tetrahydroisoquinoline derivatives. A molecular modeling study of compound **21a** was performed to elucidate its possible binding modes and to provide a structural basis for the further structure-guided design of PAK4 inhibitors.

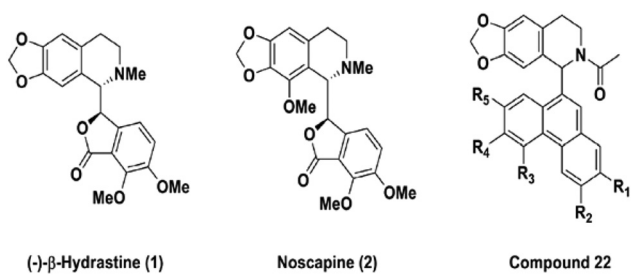

Fig. 1 Structures of (−)-β-hydrastine (**1**), noscapine (**2**) and compound **22**.

Results and discussion

Chemistry

The synthetic methods for the preparation of target compounds are summarized as follows (Scheme 1). Overall, they were prepared in 7 or 8 steps beginning with condensation of various benzaldehydes with various phenyl acetic acids to obtain **13a–o** in a *cis–trans*-isomer ratio of 90 : 10 (isolated yield). The *cis*-isomer, which was transformed into the *trans* isomer in the next esterification reaction in MeOH–H_2SO_4, did not need to be isolated. Meanwhile, some references reported that both the *cis* and *trans* esterifiable isomers could be coupled in the next reaction.[31] The intramolecular coupling reaction is the key step in the reaction of the stilbene with VOF_3, which was applied to only substrates with at least three electron donating groups providing **15a–o**.[32] The methyl esters of **15a–q** were hydrolyzed to carboxylic acids with sodium hydroxide to afford the phenanthrene-carboxylic acids **16a–o** in quantitative yield. Compounds **17a–o** and **18a–o** were synthesized by treating the phenanthrenecarboxylic acids with HOBt and EDCI in DCM at 0 °C for 2.5 h, followed by homoveratrylamine or homopiperonylamine to afford the amides after 15 min.[33] Bischler–Napieralski reaction of compounds **17a–o** and **18a–o** using phosphorus oxychloride as a cyclization reagent under neat conditions gave the intermediates dihydroisoquinolines in refluxing dimethoxyethane (DME) after 3.5 h. These intermediates were then directly used for the next step to furnish the desired **19a–o** and **20a–o** from the reaction of sodium borohydride in cooled MeOH overnight.[34] Subsequently, all the substituted 1-phenanthryl-tetrahydroisoquinolines (**19a–o** and **20a–o**), on treatment with acetyl chloride in the presence of K_2CO_3 as an acid-neutralizing reagent, delivered the expected final products **21a–o** and **22a–o** in quantitative yield. Finally, the deprotection of **21g–l** and **22g–l** in an ultrasonic reactor with 1,4-cyclohexadiene and 10% Pd/C afforded **21p–u** and **22p–u** in quantitative yield.

Enzymatic assay

In an attempt to evaluate the ability of various 1-phenanthryl-tetrahydroisoquinoline derivatives to inhibit PAK4, all the new synthetic compounds and the reference compound (−)-β-hydrastine (**1**) were initially assayed for their inhibitory effects against PAK4 using Kinase Glo® Luminescent Kinase Assays, and compounds with high potency for PAK4 were selected for further profiling (Table 1). The reported IC_{50} values are the average of at least three independent experiments.

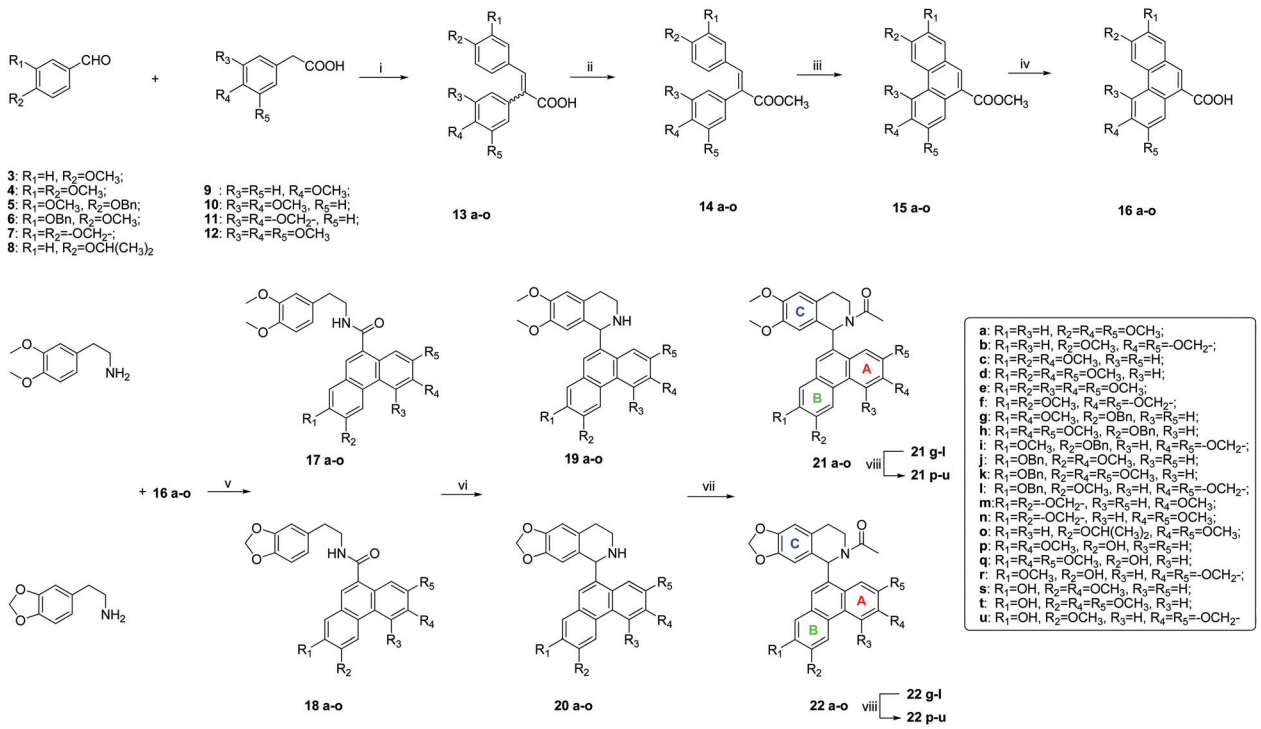

Scheme 1 Reagents and conditions: (i) (a) Ac_2O, Et_3N, reflux, 10 h; (b) NaOH (aq.), 2 h; (ii) H_2SO_4, MeOH, reflux, 4 h; (iii) VOF_3, DCM, EtOAc, TFA, TFAA, ice-salt bath, 1.5 h; (iv) NaOH, MeOH–H_2O or THF–H_2O, reflux; (v) (a) EDCI, HOBt, DCM, 0 °C; (b) DIPEA, phenethylamine, rt; (vi) (a) $POCl_3$, DME, reflux; (b) $NaBH_4$, MeOH, 0 °C; (vii) acetyl chloride, TEA, DCM, 0 °C; (viii) 1,4-cyclohexadiene, DCM–MeOH, 10% Pd/C, ultrasound, 25 °C, 100 min.

Table 1 Inhibitory effects of new compounds against PAK4 kinase[a]

Compound	PAK4 (IC_{50}, μM)	Purity%	Compound	PAK4 (IC_{50}, μM)	Purity%
21a	8.84 ± 0.09	99.39	**22a**	8.76 ± 0.04	99.64
21b	10.17 ± 0.12	99.76	**22b**	10.74 ± 0.29	99.53
21c	9.87 ± 0.47	95.52	**22c**	9.96 ± 0.46	95.56
21d	13.44 ± 0.19	99.54	**22d**	17.67 ± 0.15	99.30
21e	8.47 ± 0.15	98.59	**22e**	12.23 ± 0.33	97.69
21f	14.47 ± 0.26	98.95	**22f**	16.51 ± 0.20	99.84
21g	9.66 ± 0.11	97.21	**22g**	10.95 ± 0.17	95.38
21h	11.70 ± 0.07	99.88	**22h**	12.49 ± 0.12	98.74
21i	9.97 ± 0.03	99.61	**22i**	9.85 ± 0.13	98.42
21j	10.17 ± 0.05	99.71	**22j**	10.48 ± 0.21	97.51
21k	12.25 ± 0.06	99.45	**22k**	11.25 ± 0.10	99.40
21l	8.61 ± 0.08	97.12	**22l**	9.52 ± 0.03	98.58
21m	10.81 ± 0.14	100.00	**22m**	12.79 ± 0.03	99.72
21n	9.90 ± 0.15	99.70	**22n**	15.86 ± 0.25	98.72
21o	8.01 ± 0.06	99.18	**22o**	13.21 ± 0.18	99.05
21p	16.58 ± 0.18	99.55	**22p**	15.44 ± 0.11	100.00
21q	14.31 ± 0.12	98.08	**22q**	13.63 ± 0.22	99.50
21r	10.36 ± 0.08	99.55	**22r**	11.27 ± 0.07	99.55
21s	12.06 ± 0.06	95.47	**22s**	11.40 ± 0.12	98.94
21t	11.28 ± 0.03	97.10	**22t**	11.89 ± 0.08	95.48
21u	10.02 ± 0.05	99.76	**22u**	9.93 ± 0.04	99.53
PF-3758309[b]	0.028 ± 0.006		Staurosporine[b]	0.011 ± 0.008	

[a] IC_{50}s were calculated by the Logit method from the results of at least three independent tests with eleven concentrations each and expressed as the means ± SD. [b] Used as a positive control.

As shown in Table 1, most of the target compounds showed moderate-to-good inhibitory effects against PAK4, with potencies in the 5–20 μM range, indicating that the introduction of the phenanthryl ring moiety as a suitable rigid scaffold to fit into the large pocket of PAK4 increased the inhibition of kinase activity. In the ring-C modification, similar activity was observed for compounds **21a–o** and **22a–o**, which contain two methoxy groups and a methylene-dioxy group, respectively. In

our previous docking study, it was shown that the substitutions on the tetrahydroisoquinoline part do not have much impact on the interactions with PAK4, primarily due to this part much more exposed to the solvent than any other parts. When ring-A was replaced with C-3-methoxy, C-2,3-dimethoxy, C-2,3,4-trimethoxy, and C-2,3-methylene-dioxy substituents, compounds **21a**, **22h**, **21k**, **21n** and **22o**, which contained the C-2,3-dimethoxy group, showed higher activities. The different activities of the compounds with multiple substitution effects in ring-B demonstrated that the modification of ring-B was crucial. A comparison of compounds **21a**, **21c**, **21h**, and **21o** revealed a substitution effect at C-6 of ring-B. Compound **21o**, which contains an isopropoxy group, showed the most potent activity against PAK4, with an IC_{50} value of 8.0 μM. The conversion of the C-6-OiPr to C-6-OMe (**21a**) resulted in a tiny decrease in potency, with an IC_{50} value of 8.8 μM. The addition of an extra benzyloxy group or methoxy group at C-7, as in compound **21d** or **21k**, respectively, led to a decrease in biological activity. When the C-6-OMe and C-7-OBn were changed, the anti-kinase activities of compounds **21h** and **21k** had no significant change. In the ring-B modification, the deprotection of the benzyl to give an –OH group, accompanied by a C-6-OMe or C-7-OMe, was found to decrease the biological activity, indicating that the hydrogen bond donating OH group is disfavoured. Consequently, this finding indicates that the combination of C-2,3-dimethoxy-6-isopropoxyphenanthryl or C-2,3,6-trimethoxyphenanthryl is the most favourable modification for the anti-proliferative activity of 1-phenanthryl-tetrahydroisoquinoline analogues.

Cellular inhibition study

Based on the enzymatic assay, potent inhibitors were selected for the cellular assay. The antiproliferative effects of the compounds listed in Table 2 are in the MCF-7 cell line and the A549 cell line, in which PAK4 has been found to be overexpressed. Meanwhile, the tumour cell line HT-1080 whose growth was not dependent on PAK4, was used to test the potential off-target effects of the potent PAK4 inhibitors. In parallel with the enzymatic results, all the selected compounds displayed antiproliferative effects in the MCF-7 and A549 cell lines. Compound **21a** bearing a C-6-OMe group in ring-B, showed IC_{50} values of 0.85 μM and 1.35 μM in the MCF-7 and the A549 cells respectively, and a 40-fold selectivity over HT1080 cells. Compounds **21i**, **21l**, and **21o** were found to decrease the biological activity. Compound **22u**, bearing an –OH group, showed high potency with IC_{50} values of 0.92 μM and 0.72 μM in the MCF-7 and A549 cells respectively. Meanwhile, compound **22u** also showed high potency in the HT1080 cells, indicating that general cytotoxicity might exist. Quite disappointingly, compound **21o** showed less potent activity in the MCF-7 cell line compared with **21a**.

Table 2 Inhibitory effects of potent compounds on cell proliferation

Compound	PAK4 (IC_{50}, μM)	IC_{50}[a] (μM)		
		MCF-7	A549	HT1080
21a	8.84	0.85	1.35	>50
21c	9.88	6.63	5.28	15.89
21e	8.47	4.22	>30	34.00
21i	9.97	7.81	2.33	27.29
21l	8.61	5.08	3.86	31.80
21o	8.01	5.04	8.03	45.76
22u	9.93	0.92	0.72	4.71

[a] IC_{50}: concentration of the compound (μM) displaying 50% cell growth inhibition after 24 h of drug exposure, as determined by the MTT assay. Each experiment was carried out in triplicate.

Cell cycle analysis

We next examined the effect of compound **21a** on the proliferation of human cancer cells. As shown in the MTT assay, treatment with compound **21a** inhibited the proliferation of MCF-7 and A549 cells at 1 μM. To investigate the mechanism by which compound **21a** inhibited the growth of human breast cancer cells, we explored the effects of compound **21a** on cell-cycle distribution by flow cytometry. After 24 h of exposure, compound **21a** was found to induce an increase in the percentage of cells in the G1 phase and decrease in the S phase compared with the vehicle control, indicating that compound **21a** arrests MCF-7 cells at the G1 phase of the cell cycle (Fig. 2A). Since cyclin D1/3 and CDK2/4/6 are key regulators in the G1 phase of the cell cycle, we then examined the expression level of these factors along with the level of activated PAK4-(phospho-Ser474) in compound **21a** treated cancer cells. Western blot analysis found that exposure of MCF-7 to compound **21a** (5 and 10 μM) for 24 h dramatically decreased levels of phospho-PAK4, CDK2, CDK4, CDK6, cyclin D1 protein, and cyclin D3 protein expression in a dose-dependent manner (Fig. 2B). All these data demonstrate that compound **21a** suppresses the proliferation of breast cancer cells and mediates cell cycle arrest *via* repression of cyclin D and CDKs.

Compound 21a induces apoptosis in breast cancer cells

We further tested whether apoptosis induction could contribute to the growth inhibitory function of **21a** in MCF-7 cells. The ability of **21a** to induce apoptosis in MCF-7 cells was thus evaluated by the treatment of cells with **21a** for 24 h and subsequently subjecting the cells to staining with annexin V and propidium iodide (PI), and flow cytometry analysis. As shown in Fig. 3, treatment with **21a** (0 μM, 5 μM, and 10 μM) for 24 h caused 13.3% annexin V-positive cells compared with controls, which showed only 5.7% annexin V-positive cells (Fig. 3A). The results indicate that **21a** can induce apoptosis in breast cancer cells. To elucidate the molecular mechanisms involved in the observed apoptosis alterations, we detected the expression of several apoptosis regulators in **21a** treated cancer cells. Results showed that **21a** decreased the levels of phospho-PAK4 and Bcl-2, increased BAX, caspase 3, and caspase 8 expression in MCF-7 cells (Fig. 3B). Above data indicate that **21a** induces apoptosis of breast cancer cells *via* affecting indicated apoptosis regulators along with the inhibition of PAK4 kinase activity.

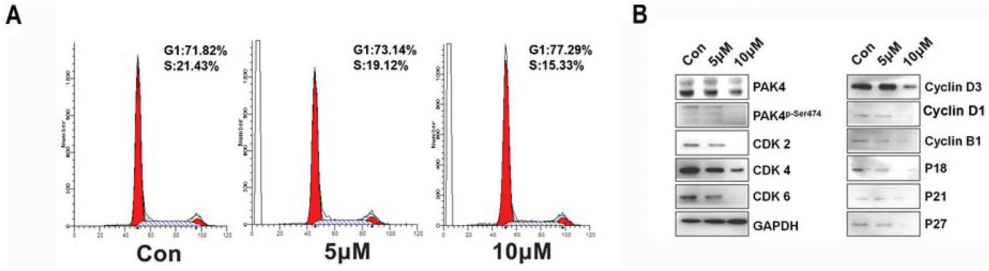

Fig. 2 Compound **21a** affects cell cycle distribution in MCF-7 cancer cells. (A) Untreated cells (control) and cells treated with compound **21a** at different concentrations for 24 h; (B) **21a** downregulates the expression level of cyclin D and CDKs.

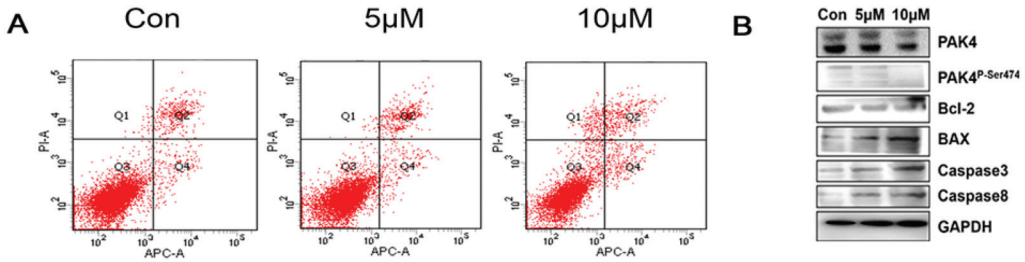

Fig. 3 The effect of **21a** on apoptosis of breast cancer cells. (A) Untreated cells (control) and cells treated with compound **21a** at different concentrations for 24 h; (B) **21a** downregulates Bcl-2 expression and upregulates BAX, caspase 3, and caspase 8.

Cell migration and invasion assay

PAK4 activity is involved in cytoskeleton dynamics and cancer cell migration and invasion, therefore, the inhibitory effect of **21a** on breast cancer cell migration and invasion were analysed. By Transwell assay, a dose-dependent decrease in cell migration and invasion was observed following treatment with compound **21a** (Fig. 4A). As reported, PAK4-regulated cell migration and invasion *via* the PAK4/LIMK1/cofilin, PAK4/MMP2, or PAK4/SCG10 signaling pathway. Here, the effects of compound **21a** on the PAK4/LIMK1/cofilin, PAK4/MMP2, or PAK4/SCG10 signaling pathways were examined by Western blot analysis. As we expected, exposure of MCF-7 cells with different concentrations of compound **21a** for 24 h inhibited the levels of activated PAK4, phosphor-LIMK1, phosphor-cofilin, and phosphor-SCG10 phosphorylation in a dose-dependent manner (Fig. 4B), indicating that the mechanism of **21a** repressing breast cancer cell migration and invasion correlates with **21a** inhibiting PAK4 kinase activity and its certain downstream substrates.

Lentivirus production and infection

To further clarify whether the regulation of **21a** on MCF-7 migration and invasion depend on its inhibitory effect of PAK4 kinase activity, we stably transfected Flag-tagged PAK4WT (wild type PAK4) or PAK4KM (kinase dead PAK4) into MCF-7 cells and then performed Transwell assay following treatment with **21a**. As a result, PAK4WT-overexpressed cells showed an enhanced-inhibitory effect by **21a** on both migration and invasion of MCF-7 cells compared to vector control, while PAK4KM did not. Furthermore, treatment with compound **21a** exhibited a significantly reduced inhibition of the invasive and migratory effects in PAK4 silenced cells, which were transfected with sh-PAK4 recombinant lentivirus (Fig. 5B). Further, we detected PAK4 activity and its substrates' phosphorylation level in PAK4WT overexpressed cells or PAK silenced cells by western blot assay. Data showed the same results with the migration and invasion assays (Fig. 5C). All these experiments demonstrated that compound **21a** represses the invasive and migratory capacity of MCF-7 cells *via* inhibiting PAK4 kinase activity.

Molecular modelling

To investigate the mechanism by which compound **21a** interacts with PAK4, we performed a docking study between **21a** and PAK4. Both isomers of **21a** were studied. The crystal structure of PAK4 in complex with PF3758309 (PDB entry code: 2X4Z)[23] was used as the receptor. Molecular docking was carried out using Glide XP (Schrodinger 2014). The ligand poses that Glide generated passed through a series of hierarchical filters that evaluated the ligand's interaction with the receptor. The final binding model is shown in Fig. 6.

In 2014, Li *et al.*[35] constructed a ligand-based pharmacophore model for PAK4 inhibitors consisting of five chemical features: a positive ionizable center, two hydrophobic groups, a hydrogen donor, and a hydrogen acceptor. It was demonstrated that the crucial anchoring points inside the binding site include Glu396, Phe397, and Leu398 which play important roles in the affinity of PAK4 inhibitors. The other anchoring point is the conserved water molecule W2142 including

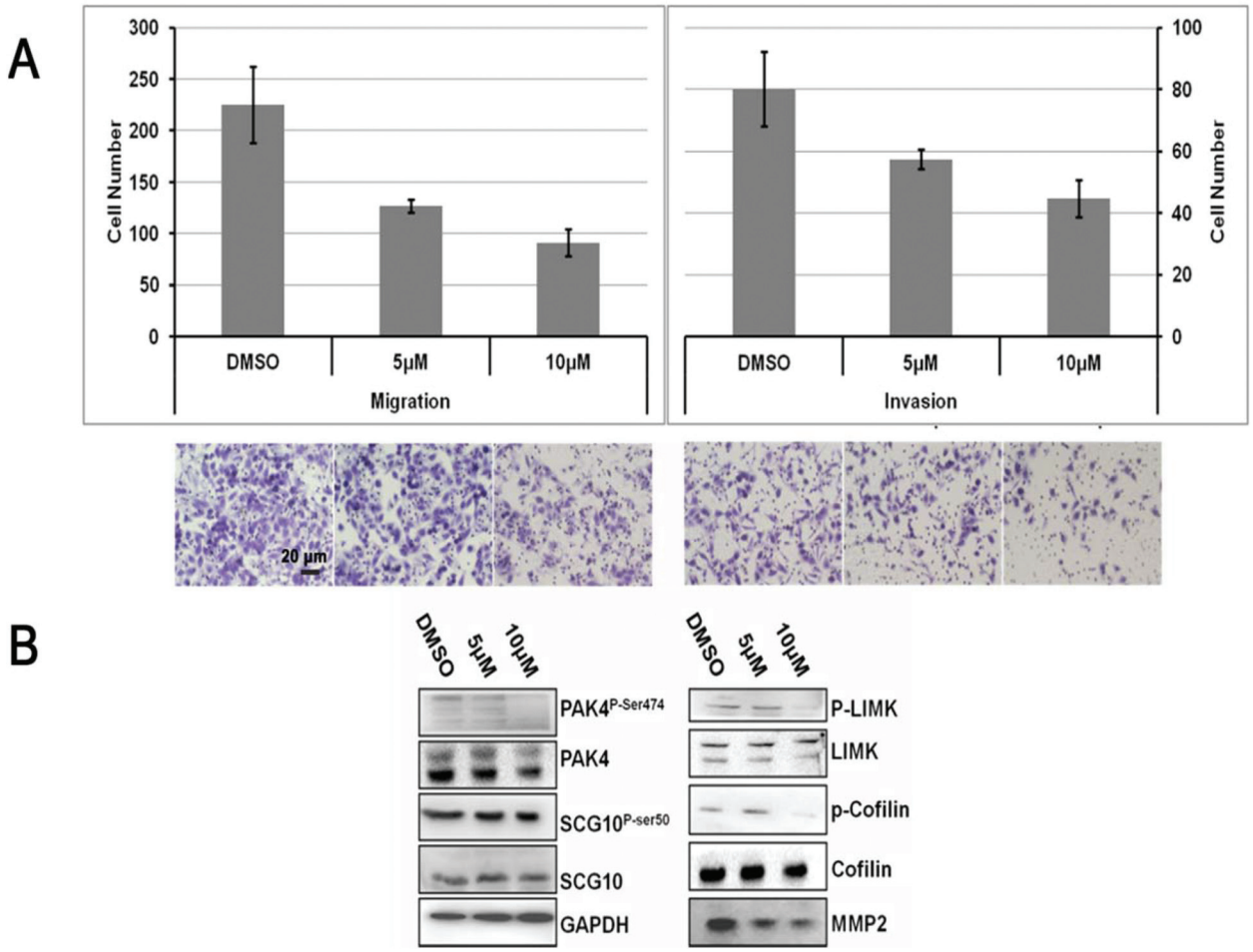

Fig. 4 **21a** suppresses the migration and invasion of human breast cancer cells and inhibits the PAK4/LIMK1/cofilin and PAK4/SCG10 signaling pathways. (A) MCF-7 cells migratory and invasive capacities were evaluated by using a Boyden chamber matrigel invasion assay. After 24 h of treatment with the indicated concentrations of **21a**, the invaded cells were fixed and stained, and 10 random fields were counted. (B) Western blot analysis shows the protein level of the proteins involved in migration and invasion.

Asp458 and Lys350 which influences PAK4 selectivity. In Fig. 6, both isomers of compound **21a** bind to the PAK4 catalytic domain fairly well. The bulky and lipophilic phenanthrene group makes effective hydrophobic interactions with the highly hydrophobic ATP binding site.[36,37] In particular, compound (*R*)-**21a** makes hydrogen bonds with a conserved water molecule and a protein residue Glu329 while compound (*S*)-**21a** makes hydrogen bonds with protein residues (Glu396, Ile327, Ala402). This model suggests that hydrophobic interactions play an important role between the compound and PAK4 and they offer a structural explanation for the activity of the compound.

Experimental

Chemistry

General chemistry methods. Unless otherwise noted, all materials were obtained from commercially available sources and were used without purification. TLC was performed on silica gel plates (thickness 250 mm, Indicator F-254) and visualized by UV-light. ^{1}H NMR and ^{13}C NMR spectra were recorded using a Bruker 400 MHz NMR spectrometer in DMSO-d_6 and $CDCl_3$, respectively and the chemical shifts were recorded in parts per million downfield from TMS. High resolution accurate mass determinations (HRMS) for all final target compounds were obtained using a Bruker Micromass Time of Flight mass spectrometer equipped with electrospray ionisation (ESI). Column chromatography was performed with silica gel (200–300 mesh) purchased from Qingdao Haiyang Chemical Co. Ltd. The purities of compounds used for biological evaluation (>95%) were determined using a Waters 2000 HPLC system: column, Unitary C18, 4.6 mm × 250 mm, 5 μm; solvent A = H_2O, solvent B = MeOH; flow rate, 1.0 mL min^{-1}. Samples were eluted with a gradient of 70% MeOH–H_2O to 95% MeOH–H_2O over 15 min and detected at 254 nm.

General synthetic procedure for the preparation of 13a–o. A solution of substituted phenylacetic acid (7.5 mmol), substituted benzene formaldehyde (7.5 mmol), acetic anhydride (3 mL), and triethylamine (1.5 mL) was refluxed with stirring

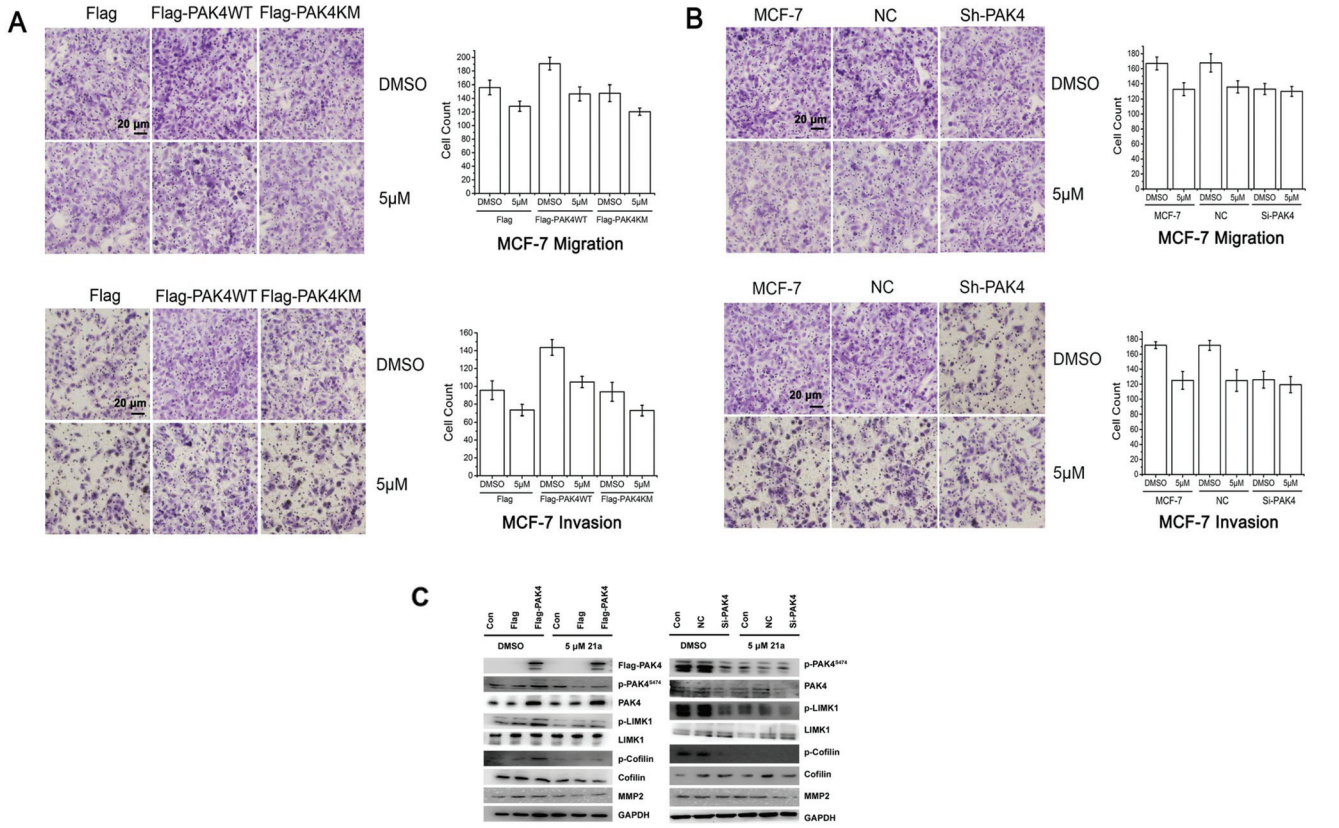

Fig. 5 **21a** suppresses migration and invasion of human breast cancer cells *via* PAK4 kinase activity. (A) The migratory and invasive capacities PAK4WT/KM stable transfected MCF-7 cells of $PAK4^{Wt}$ and $PAK4^{KM}$ MCF-7 cells were evaluated by using a Boyden chamber matrigel invasion assay. (B) $PAK4^{Si}$ MCF-7 cells migratory and invasive capacities were evaluated. (C) Western blot analysis shows the protein levels involved in migration and invasion in PAK4-overexpressed or PAK4-silenced cells.

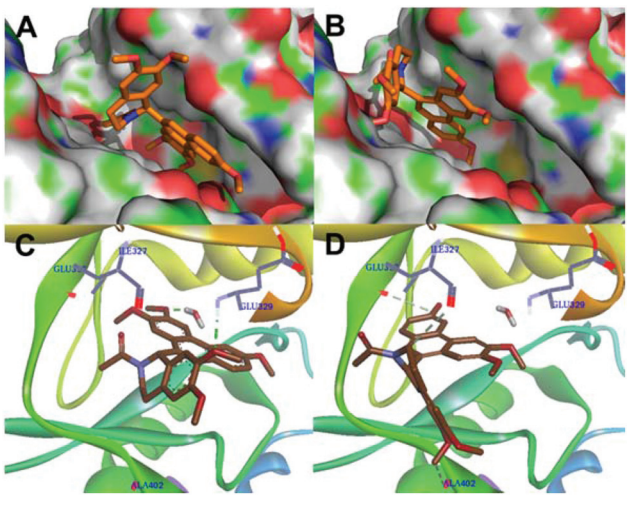

Fig. 6 Predicted binding modes of PAK4 in complex with the most active compound **21a**. PAK4 is shown in a cartoon representation with the bound inhibitor in a stick representation. The gray dots indicate potential hydrogen bonds between the compound and PAK4. (A) Space matching of compound (*R*)-**21a**. (B) Space matching compound (*S*)-**21a**. (C) Best docking pose of compound (*R*)-**21a**. (D) Best docking pose of compound (*S*)-**21a**.

under N_2 for 10 h. The resulting solution was cooled to room temperature, 10% NaOH solution (25 mL) was added, and then the resulting mixture was stirred for 2 h at 90 °C. The reaction mixture was cooled to room temperature and neutralized with concentrated HCl (pH 3). The yellow stilbene acid obtained was collected by filtration and recrystallized from acetonitrile to yield pure **13a–o** as yellow needles. For example:

*(E/Z)-2-(3,4-Dimethoxyphenyl)-3-(4-methoxyphenyl)-acrylic acid (**13a**).* Yellow needle, yield: 73%. mp 214.1–215.5 °C. ^{1}H NMR (400 MHz, DMSO-d_6) δ 12.43 (s, 1H), 7.67 (s, 1H), 7.06–7.04 (d, J = 8.84 Hz, 2H), 6.98–6.96 (d, J = 8.24 Hz, 1H), 6.80–6.78 (d, J = 8.88 Hz, 2H), 6.74–6.73 (d, J = 1.88 Hz, 1H), 6.68–6.66 (dd, J = 8.12, 1.88 Hz, 1H), 3.78 (s, 1H), 3.71 (s, 1H), 3.66 (s, 1H). ^{13}C NMR (100 MHz, DMSO-d_6) δ 169.22, 160.32, 149.26, 148.67, 138.98, 132.42(×2), 131.00, 129.40, 127.47, 122.20, 114.29(×2), 113.63, 112.40, 56.00, 55.90, 55.63. MS (ESI) m/z 315.2 $[M + H]^+$, 337.2 $[M + Na]^+$, 353.1 $[M + K]^+$.

General synthetic procedure for the preparation of 14a–o. Stilbene acid **13a–o** (5 mmol) was dissolved in MeOH (15 mL) containing concentrated H_2SO_4 (0.1 mL) and the resulting solution was refluxed for 6 h and then cooled to room temperature overnight. The mixture was filtered and the solid was washed twice with cooled MeOH. The solid was dried in a vacuum to give **14a–o**. The filtrate was evaporated under

reduced pressure; water was added. The mixture was extracted with CH_2Cl_2 and brine. The organic phase was dried over Na_2SO_4 overnight and the solvent was removed in a vacuum. The oil was purified by silica gel column chromatography (*n*-hexane–EtOAc as an eluent) to afford an addition of **14a–o** as off-yellow crystals. For example:

*Z-2-(3,4-Dimethoxyphenyl)-3-(4-methoxyphenyl)-acrylic acid methyl ester (**14a**).* Off-yellow needle, yield: 74%. mp 110.6–111.7 °C. ^{1}H NMR (400 MHz, $CDCl_3$) δ 7.78 (s, 1H), 7.03–7.01 (d, J = 8.88 Hz, 1H), 6.91–6.89 (d, J = 8.20 Hz, 1H), 6.80–6.77 (dd, J = 8.16, 1.88 Hz, 1H), 6.74–6.73 (d, J = 1.88 Hz, 1H), 6.71–6.68 (d, J = 8.88 Hz, 2H), 3.93 (s, 1H), 3.80 (s, 1H), 3.79 (s, 1H), 3.76 (s, 1H). ^{13}C NMR (100 MHz, $CDCl_3$) δ 168.74, 160.29, 149.14, 148.58, 140.17, 132.40(×2), 129.62, 128.66, 127.30, 122.12, 113.72(×2), 112.86, 111.45, 55.89, 55.82, 55.22, 52.29. MS (ESI) m/z 329.2 $[M + H]^+$, 351.2 $[M + Na]^+$, 367.1 $[M + K]^+$.

General synthetic procedure for the preparation of 15a–o. A solution composed of stilbene ester **14a–o** (2.5 mmol) was dissolved in dry CH_2Cl_2 (8 mL) containing trifluoroacetic acid (0.2 mL) and trifluoroacetic anhydride (0.04 mL). A solution of vanadium oxytrifluoride (5 mmol) in CH_2Cl_2 (6.5 mL) and EtOAc (3.5 mL) was added dropwise. During the addition (90 min), the reaction mixture was cooled in an ice-salt bath. The dark brown mixture was stirred for an additional 0.5 h in an ice-salt bath, then poured onto crushed ice, and was extracted with CH_2Cl_2. The organic layer was washed with brine, dried over Na_2SO_4, and concentrated under reduced pressure. The residue was purified by silica gel column chromatography ($CHCl_3$ as an eluent) to afford **15a–o** as white solids. For example:

*3,6,7-Trimethoxyphenanthrene-9-carboxylic acid methyl ester (**15a**).* White solid, yield: 87%. mp 151.2–152.0 °C. ^{1}H NMR (400 MHz, $CDCl_3$) δ 8.65 (s, 1H), 8.44 (s, 1H), 7.87 (s, 1H), 7.86–7.84 (d, J = 8.80 Hz, 1H), 7.81–7.80 (d, J = 2.24 Hz, 1H), 7.23–7.20 (dd, J = 8.76, 2.40 Hz, 1H), 4.11 (s, 1H), 4.09 (s, 1H), 4.03 (s, 1H), 4.01 (s, 1H). ^{13}C NMR (100 MHz, $CDCl_3$) δ 168.24, 160.20, 149.94, 148.91, 133.43, 131.87, 131.29, 125.19, 124.99, 124.27, 121.68, 116.03, 106.97, 103.75, 103.25, 55.92, 55.88, 55.55, 52.02. MS (ESI) m/z 327.2 $[M + H]^+$, 349.2 $[M + Na]^+$, 325.1 $[M - H]^-$.

General synthetic procedure for the preparation of 16a–o. **15a–o** (3 mmol) and NaOH (18 mmol) were dissolved in MeOH (9 mL) and water (9 mL) and refluxed for 4 h. On cooling, the solvent was neutralized with concentrated HCl (pH 2). The crude solids were filtered, washed with water, and dried under vacuum for 12 h to give **16a–o** as white solids. For example:

*3,6,7-Trimethoxyphenanthrene-9-carboxylic acid (**16a**).* White solid, yield: 98%. mp 213.0–214.6 °C. ^{1}H NMR (400 MHz, DMSO-d_6) δ 12.94 (s, 1H), 8.58 (s, 1H), 8.45 (s, 1H), 8.14 (s, 1H), 8.11–8.10 (d, J = 2.16 Hz, 1H), 8.05–8.03 (d, J = 8.84 Hz, 1H), 7.30–7.27 (dd, J = 8.76, 2.32 Hz, 1H), 4.06 (s, 3H), 4.04 (s, 3H), 3.92 (s, 3H). ^{13}C NMR (100 MHz, DMSO-d_6) δ 169.40, 160.41, 149.98, 149.30, 133.30, 132.16, 130.78, 125.19, 124.98, 124.26, 117.03, 107.29, 104.86, 104.55, 56.32, 56.15, 55.71. MS (ESI) m/z 310.9 $[M - H]^-$.

General synthetic procedure for the preparation of 17a–o and 18a–o. A solution of **16a–o** (2 mmol), EDCI (3 mmol) and HOBt (3 mmol) in dry CH_2Cl_2 (6 equiv.) was stirred at 25 °C for 3.5 h. Then substituted phenethylamine (2 mmol) and DIPEA (4 mmol) were added and the reaction was stirred at the same temperature for another 1.5 h. The organic layer was washed with water and brine and dried over Na_2SO_4. Removal of the solvent gave a residue that was purified by column chromatography (silica gel, CH_2Cl_2–acetone 20 : 1 as an eluent) to furnish **17a–o** or **18a–o** as white solids. For example:

*N-(3,4-Dimethoxyphenethyl)-2,6,7-trimethoxyphenanthrene-9-carboxamide (**17a**).* White solid, yield: 82%. mp 149.8–151.5 °C. ^{1}H NMR (400 MHz, $CDCl_3$) δ 7.89 (s, 1H), 7.86 (s, 1H), 7.81–7.80 (d, J = 2.28 Hz, 1H), 7.73–7.71 (d, J = 8.76 Hz, 1H), 7.21–7.18 (dd, J = 8.76, 2.28 Hz, 1H), 7.60 (s, 1H), 6.83 (s, 2H), 6.82 (s, 1H), 6.17–6.14 (t, J = 5.68 Hz, 1H), 4.11 (s, 3H), 4.03 (s, 3H), 4.02 (s, 3H), 3.87 (s, 3H), 3.85 (s, 3H), 3.78–3.38 (q, J = 13.16, 6.90 Hz, 2H), 3.00–2.96 (t, J = 6.80 Hz, 2H). ^{13}C-NMR (100 MHz, $CDCl_3$) δ 170.05, 159.30, 149.73, 149.29, 149.13, 132.02, 131.35, 130.68, 129.82, 124.88, 124.52, 124.38, 124.25, 120.77, 115.98, 112.06, 111.45, 106.49, 103.84, 103.30, 55.99, 55.94(×2), 55.88, 55.54, 41.22, 35.30. MS (ESI) m/z 475.2 $[M + H]^+$.

General synthetic procedure for the preparation of 19a–o and 20a–o. To a solution of **17a–o** or **18a–o** (1 mmol) in dimethoxymethane (5 mL) in a round-bottom flask was added phosphorus oxychloride (2 mL) and the resulting mixture was refluxed for 3.5 h. The reaction was then cooled to 0 °C for 1 h and the solution was filtered to afford the dihydroisoquinoline. These compounds were found to be unstable and decompose on standing or exposure to silica gel. They were therefore reacted without further purification immediately. To a solution of the dihydroisoquinoline in MeOH (5 mL) at 0 °C, sodium borohydride (37.8 mg) was added slowly. The resulting mixture was stirred for 1.5 h at 0 °C and a brine solution was added and then extracted with DCM. The amine was then purified by column chromatography (TEA neutralized silica gel, CH_2Cl_2–MeOH 20 : 1 as an eluent) to furnish **19a–o** or **20a–o** as white solids. For example:

*6,7-Dimethoxy-1-(3,6,7-trimethoxyphenanthren-9-yl)-1,2,3,4-tetrahydroisoquinoline (**19a**).* White solid, yield: 63% (for 2 steps). mp 270.5–272.8 °C. ^{1}H NMR (400 MHz, $CDCl_3$) δ 8.06 (s, 1H), 8.06–8.05 (d, J = 2.24 Hz, 1H), 7.79–7.77 (d, J = 8.72 Hz, 1H), 7.71 (s, 1H), 7.44 (s, 1H), 7.20–7.17 (dd, J = 8.72, 2.24 Hz, 1H), 6.80 (s, 1H), 6.20 (s, 1H), 5.58 (s, 1H), 4.13 (s, 3H), 4.13–4.09 (q, 1H), 4.00 (s, 3H), 3.99 (m, 3H), 3.74 (s, 3H), 3.68 (s, 3H), 3.17–3.15 (m, 4H), 3.00–2.97 (m, 1H), 2.79–2.75 (m, 1H). ^{13}C NMR (100 MHz, $CDCl_3$) δ 158.53, 148.76, 148.57, 147.82, 147.36, 131.13, 130.45(×2), 127.97, 126.80, 126.00, 125.50, 125.37(×2), 116.26(×2), 112.47, 111.00, 104.74, 104.53, 56.26, 55.99(×2), 55.93, 55.86, 55.37, 49.06, 29.39. MS (ESI) m/z 460.3 $[M + H]^+$, 482.3 $[M + Na]^+$.

General synthetic procedure for the preparation of 21a–o and 22a–o. A solution of **19a–o** or **20a–o** (0.5 mmol) in dry acetone (5 mL) in a round-bottom flask was cooled to 0 °C and then acetyl chloride (35 μL) was added. The mixture was

stirred for 3.5 h at 0 °C and then water was added. The organic layer was washed with water and brine and dried over Na_2SO_4 overnight. Removal of the solvent gave a residue that was purified by column chromatography (silica gel, CH_2Cl_2–acetone 20 : 1 as an eluent) to furnish **21a–o** or **22a–o** as white solids. For example:

*1-(6,7-Dimethoxy-1-(3,6,7-trimethoxyphenanthren-9-yl)-3,4-dihydroisoquino-in-2-(1H)-yl)ethanone (**21a**).* White solid, 221 mg, yield: 96%. ^{1}H NMR (400 MHz, $CDCl_3$) δ 8.24 (s, 1H), 7.95 (s, 1H), 7.87–7.86 (d, J = 2.28 Hz, 1H), 7.60–7.58 (d, J = 8.76 Hz, 1H), 7.47 (s, 1H), 7.16–7.13 (dd, J = 8.76, 2.28 Hz, 1H), 6.91 (s, 1H), 6.75 (s, 1H), 6.61 (s, 1H), 4.15 (s, 3H), 4.14 (s, 3H), 4.03 (s, 3H), 3.97 (s, 3H), 3.76 (s, 3H), 3.69–3.63 (m, 1H), 3.55–3.47 (m, 1H), 3.13–3.04 (m, 1H), 2.86–2.81 (m, 1H), 2.21 (s, 3H). ^{13}C NMR (100 MHz, $CDCl_3$) δ 169.15, 158.57, 149.88, 148.90, 147.67, 133.25, 131.02, 148.26, 130.51, 127.88, 126.68, 128.46, 126.41, 125.03, 124.56, 115.19, 111.49, 111.20, 106.17, 103.85, 103.56, 56.71, 56.03, 55.95, 55.85, 55.58, 52.81, 39.46, 28.37, 21.53. HRMS calcd for $C_{30}H_{31}NO_6Na$, $[M + Na]^+$, 524.2044; found 524.2063.

*1-(6,7-Dimethoxy-1-(2-methoxyphenanthro[3,2-d][1,3]dioxol-6-yl)-3,4-dihydroisoquinolin-2(1H)-yl)ethanone (**21b**).* White solid, 206 mg, yield: 92%. ^{1}H NMR (600 MHz, $CDCl_3$) δ 8.22 (s, 1H), 7.99 (s, 1H), 7.80–7.79 (d, J = 2.04 Hz, 1H), 7.56–7.55 (d, J = 8.70 Hz, 1H), 7.38 (s, 1H), 7.14–7.11 (dd, J = 8.70, 2.22 Hz, 1H), 6.91 (s, 1H), 6.73 (s, 1H), 6.55 (s, 1H), 6.14–6.12 (d, J = 12.90 Hz, 2H), 4.00 (s, 3H), 3.95 (s, 1H), 3.73 (s, 3H), 3.66–3.63 (m, 1H), 3.52–3.47 (m, 1H), 3.09–3.03 (m, 1H), 2.84–2.80 (m, 1H), 2.21 (s, 3H). ^{13}C NMR (150 MHz, $CDCl_3$) δ 169.11, 158.51, 148.36, 148.14, 147.63, 147.56, 133.68, 131.21, 130.32, 128.50, 127.97, 127.87, 126.34, 126.25, 124.93, 116.18, 111.32, 111.08, 103.41, 103.10, 101.39, 100.82, 55.86, 55.75, 55.41, 52.79, 39.48, 28.21, 21.64. HRMS calcd for $C_{29}H_{27}NO_6Na$ $[M + Na]^+$, 508.1731; found 508.1732.

*1-(6,7-Dimethoxy-1-(2,3,6-trimethoxyphenanthren-9-yl)-3,4-dihydroisoquinolin-2(1H)-yl)ethanone (**21c**).* White solid, 209 mg, yield: 95%. ^{1}H NMR (400 MHz, $CDCl_3$) δ 8.68–8.65 (d, J = 9.20 Hz, 1H), 7.93–7.92 (d, J = 2.40 Hz, 1H), 7.86 (s, 1H), 7.49 (s, 1H), 7.34–7.31 (dd, J = 9.16, 2.52 Hz, 1H), 6.98 (s, 1H), 6.79 (s, 1H), 6.73 (s, 1H), 6.58 (s, 1H), 4.10 (s, 3H), 4.03 (s, 3H), 3.97 (s, 3H), 3.95 (s, 3H), 3.73 (s, 3H), 3.66–3.61 (s, 1H), 3.53–3.45 (s, 1H), 3.10–3.01 (m, 1H), 2.84–2.79 (m, 1H), 2.19 (s, 3H). ^{13}C NMR (100 MHz, $CDCl_3$) δ 169.09, 158.15, 149.47, 149.39, 148.20, 147.63, 134.85, 131.65, 128.03, 127.35, 127.22, 126.51, 126.38, 125.00, 124.19, 115.24, 111.54, 111.21, 108.71, 104.77, 103.24, 56.10, 55.94(×2), 55.86, 55.55, 52.56, 39.63, 28.35, 21.67. HRMS calcd for $C_{30}H_{31}NO_6Na$, $[M + Na]^+$, 524.2044; found 524.2048.

*1-(6,7-Dimethoxy-1-(2,3,6,7-tetramethoxyphenanthren-9-yl)-3,4-dihydroisoquinolin-2(1H)-yl)ethanone (**21d**).* White solid, 237 mg, yield: 96%. ^{1}H NMR (400 MHz, $CDCl_3$) δ 8.19 (s, 1H), 7.84 (s, 1H), 7.77 (s, 1H), 7.47 (s, 1H), 6.98 (s, 1H), 6.83 (s, 1H), 6.75 (s, 1H), 6.61 (s, 1H), 4.14 (s, 3H), 4.11 (s, 6H), 3.97 (s, 3H), 3.96 (s, 3H), 3.75 (s, 3H), 3.68–3.62 (m, 1H), 3.53–3.45 (m, 1H), 3.12–3.03 (m, 1H), 2.86–2.80 (m, 1H), 2.21 (s, 3H). ^{13}C NMR (100 MHz, $CDCl_3$) δ 169.30, 149.63, 149.24, 149.12, 148.81, 148.30, 147.72, 133.80, 127.96, 126.40, 125.53, 125.28, 124.78, 124.40, 111.59, 111.24, 108.77, 106.08, 103.12, 102.68, 56.68, 56.15, 56.09, 55.97, 55.90, 53.01, 39.73, 28.40, 21.33. HRMS calcd for $C_{31}H_{33}NO_7Na$, $[M + Na]^+$, 554.2149; found 554.2164.

*1-(6,7-Dimethoxy-1-(2,3,5,6,7-pentamethoxyphenanthren-9-yl)-3,4-dihydroisoquinolin-2(1H)-yl)ethanone (**21e**).* White solid, 233 mg, yield: 94%. ^{1}H NMR (400 MHz, $CDCl_3$) δ 9.09 (s, 1H), 8.02 (s, 1H), 7.39 (s, 1H), 6.99 (s, 1H), 6.90 (s, 1H), 6.71 (s, 1H), 6.55 (s, 1H), 6.00–5.99 (d, J = 0.90 Hz, 1H), 5.93–5.92 (d, J = 0.96 Hz, 1H), 4.08 (s, 6H), 4.05 (s, 3H), 4.00 (s, 3H), 3.97 (s, 3H), 3.90 (s, 3H), 3.61–3.60 (s, 1H), 3.48–3.42 (m, 1H), 3.06–3.00 (m, 1H), 2.81–2.78 (m, 1H), 2.17 (s, 3H). ^{13}C NMR (100 MHz, $CDCl_3$) δ 169.08, 152.14, 151.52, 148.99, 147.94, 146.96, 146.26, 142.42, 133.40, 130.01, 129.10, 128.22, 127.58, 125.74, 124.32, 119.07, 108.84, 108.34(×2), 107.42, 102.59, 100.95, 61.26, 60.49, 56.60, 55.77, 55.71, 53.05, 39.45, 28.77, 21.47. HRMS calcd for $C_{32}H_{35}NO_8Na$, $[M + Na]^+$, 584.2225; found 584.2229.

*1-(1-(2,3-Dimethoxyphenanthro[3,2-d][1,3]dioxol-6-yl)-6,7-dimethoxy-3,4-dihydroisoquinolin-2(1H)-yl)ethanone (**21f**).* White solid, 193 mg, yield: 91%. ^{1}H NMR (400 MHz, $CDCl_3$) δ 8.18 (s, 1H), 7.90 (s, 1H), 7.73 (s, 1H), 7.38 (s, 1H), 6.95 (s, 1H), 6.84 (s, 1H), 6.73 (s, 1H), 6.55 (s, 1H), 6.11–6.09 (d, J = 7.69 Hz, 2H), 4.08 (s, 3H), 3.96 (s, 3H), 3.95 (s, 3H), 3.73 (s, 3H), 3.67–3.61 (m, 1H), 3.52–3.44 (m, 1H), 3.10–3.01 (m, 1H), 2.84–2.79 (m, 1H), 2.20 (s, 3H). ^{13}C NMR (100 MHz, $CDCl_3$) δ 169.20, 149.64, 148.92, 148.28, 147.86, 147.71, 134.41, 128.12, 127.97, 126.80, 126.48, 125.29, 124.81, 111.58, 111.25, 108.48, 103.41, 102.73, 101.37, 100.35, 56.03, 55.97, 55.94, 55.88, 52.99, 39.62, 28.33, 21.60. HRMS calcd for $C_{30}H_{29}NO_7Na$, $[M + Na]^+$, 538.1836; found 538.1829.

*1-(1-(3-(Benzyloxy)-2,6-dimethoxyphenanthren-9-yl)-6,7-dimethoxy-3,4-dihydroisoquinolin-2(1H)-yl)ethanone (**21g**).* White solid, 261 mg, yield: 92%. ^{1}H NMR (400 MHz, $CDCl_3$) δ ^{1}H NMR (400 MHz, $CDCl_3$) δ 8.63–8.61 (d, J = 9.20 Hz, 1H), 7.89 (s, 1H), 7.71–7.70 (d, J = 2.44 Hz, 1H), 7.56–7.54 (d, J = 7.40 Hz, 2H), 7.47 (s, 1H), 7.41–7.37 (m, 2H), 7.33–7.27 (m, 2H), 6.99 (s, 1H), 6.78 (s, 1H), 6.73 (s, 1H), 6.56 (s, 1H), 5.38 (s, 2H), 3.98 (s, 6H), 3.95 (s, 3H), 3.73 (s, 3H), 3.65–3.59 (m, 1H), 3.52–3.44 (m, 1H), 3.09–3.00 (m, 1H), 2.83–2.78 (m, 1H), 2.18 (s, 3H). ^{13}C NMR (100 MHz, $CDCl_3$) δ 169.09, 150.08, 148.40, 148.25, 147.68, 137.08, 135.00, 131.61, 128.70(×2), 128.05(×2), 127.36(×2), 127.28, 127.14, 126.69, 126.47, 124.91, 124.08, 115.74, 111.58, 111.24, 108.98, 106.55, 104.21, 71.50, 55.99, 55.97, 55.87, 55.42, 52.59, 39.63, 28.37, 21.62. HRMS calcd for $C_{36}H_{35}NO_6Na$, $[M + Na]^+$, 600.2357; found 600.2349.

*1-(1-(3-(Benzyloxy)-2,6,7-trimethoxyphenanthren-9-yl)-6,7-dimethoxy-3,4-dihydroisoquinolin-2(1H)-yl)ethanone (**21h**).* White solid, 273 mg, yield: 95%. ^{1}H NMR (400 MHz, $CDCl_3$) δ 8.17 (s, 1H), 7.78 (s, 1H), 7.60 (s, 1H), 7.57 (s, 1H), 7.55 (s, 1H), 7.44 (s, 1H), 7.41–7.37 (m, 2H), 7.33–7.30 (m, 1H), 6.99 (s, 1H), 6.81 (s, 1H), 6.74 (s, 1H), 6.59 (s, 1H), 5.39 (s, 2H), 4.09 (s, 3H), 4.06 (s, 3H), 3.98 (s, 3H), 3.95 (s, 3H), 3.74 (s, 3H), 3.65–3.61 (m, 1H), 3.50–3.42 (m, 1H), 3.10–3.01 (m, 1H), 2.83–2.78 (m, 1H), 2.18 (s, 3H). ^{13}C NMR (100 MHz, $CDCl_3$) δ 169.06, 149.35, 149.11, 149.03, 148.54, 148.26, 147.68, 137.29, 134.15, 128.70(×2),

128.03(×2), 127.76, 127.30(×2), 126.49, 125.56, 125.39, 124.72, 124.19, 111.61, 111.26, 108.97, 106.27, 106.07, 102.93, 71.70, 56.63, 55.97(×2), 55.87(×2), 52.81, 39.64, 28.39, 21.47. HRMS calcd for $C_{37}H_{37}NO_7Na$, $[M + Na]^+$, 630.2462; found 630.2461.

*1-(1-(2-(Benzyloxy)-3-methoxyphenanthro[3,2-d][1,3]dioxol-6-yl)-6,7-dimethoxy-3,4-dihydroisoquinolin-2(1H)-yl)ethanone (**21i**).* White solid, 239 mg, yield: 91%. ^{1}H NMR (400 MHz, $CDCl_3$) δ 8.15 (s, 1H), 7.78 (s, 1H), 7.74 (s, 1H), 7.54 (s, 1H), 7.52 (s, 1H), 7.41–7.36 (m, 3H), 7.33–7.29 (m, 1H), 6.97 (s, 1H), 6.83 (s, 1H), 6.72 (s, 1H), 6.54 (s, 1H), 6.09 (s, 1H), 6.07 (s, 1H), 5.35 (s, 2H), 3.96 (s, 3H), 3.94 (s, 3H), 3.72 (s, 3H), 3.65–3.60 (m, 1H), 3.51–3.43 (m, 1H), 3.09–3.01 (m, 1H), 2.83–2.78 (m, 1H), 2.20 (s, 3H). ^{13}C NMR (100 MHz, $CDCl_3$) δ 169.35, 149.47, 148.66, 148.29, 147.82, 147.72, 147.66, 136.83, 134.38, 128.68(×2), 128.04, 127.98, 127.38(×2), 126.66, 126.47, 126.36, 125.55, 124.67, 111.51, 111.22, 108.76, 105.59, 103.29, 101.34, 100.34, 77.24, 71.17, 55.97(×2), 55.86, 53.08, 39.64, 28.32, 21.46. HRMS calcd for $C_{36}H_{33}NO_7Na$, $[M + Na]^+$, 614.2150; found 614.2148.

*1-(1-(2-(Benzyloxy)-3,6-dimethoxyphenanthren-9-yl)-6,7-dimethoxy-3,4-dihydroisoquinolin-2(1H)-yl)ethanone (**21j**).* White solid, 240 mg, yield: 93%. ^{1}H NMR (400 MHz, $CDCl_3$) δ 8.67–8.65 (d, J = 9.20 Hz, 1H), 7.94–7.93 (d, J = 2.44 Hz, 1H), 7.89 (s, 1H), 7.49–7.47 (m, 3H), 7.40–7.36 (m, 2H), 7.34–7.30 (m, 2H), 7.07 (s, 1H), 6.77 (s, 1H), 6.72 (s, 1H), 6.57 (s, 1H), 5.21 (s, 2H), 4.03 (s, 3H), 3.94 (s, 3H), 3.73 (s, 3H), 3.65–3.60 (m, 1H), 3.53–3.45 (m, 1H), 3.09–3.00 (m, 1H), 2.83–2.78 (m, 1H), 2.19 (s, 3H). ^{13}C-NMR (100 MHz, $CDCl_3$) δ 169.10, 158.16, 149.92, 148.89, 148.25, 147.69, 136.70, 134.82, 131.64, 128.57(×2), 128.05, 127.95, 127.43(×2), 127.33, 127.23, 126.49, 126.39, 125.07, 124.54, 115.28, 111.61, 111.30, 110.67, 104.88, 103.91, 70.74, 56.27, 55.96, 55.87, 55.56, 52.61, 39.65, 28.36, 21.64. HRMS calcd for $C_{36}H_{35}NO_6Na$, $[M + Na]^+$, 600.2357; found 600.2359.

*1-(1-(2-(Benzyloxy)-3,6,7-trimethoxyphenanthren-9-yl)-6,7-dimethoxy-3,4-dihydroisoquinolin-2(1H)-yl)ethanone (**21k**).* White solid, 199 mg, yield: 90%. ^{1}H NMR(400 MHz, $CDCl_3$) δ 8.19 (s, 1H), 7.85 (s, 1H), 7.81 (s, 1H), 7.40–7.37 (m, 2H), 7.34–7.30 (m, 1H), 7.07 (s, 1H), 6.81 (s, 1H), 6.73 (s, 1H), 6.60 (s, 1H), 5.20 (s, 2H), 4.13 (s, 3H), 4.11 (s, 3H), 4.10 (s, 3H), 3.95 (s, 3H), 3.74 (s, 3H), 3.66–3.61 (m, 1H), 3.52–3.45 (m, 1H), 3.11–3.02 (m, 1H), 2.85–2.80 (m, 1H), 2.21 (s, 3H). ^{13}C NMR (100 MHz, $CDCl_3$) δ 169.10, 150.10, 149.23, 149.09, 148.25, 148.19, 147.68, 136.78, 133.97, 128.57(×2), 128.02, 127.93, 127.87, 127.44(×2), 126.50, 125.64, 125.31, 124.74, 124.70, 111.62, 111.29, 110.76, 106.18, 103.38, 103.15, 70.75, 56.65, 56.36, 56.09, 55.96, 55.89, 52.84, 39.67, 28.38, 21.49. HRMS calcd for $C_{37}H_{37}NO_7Na$, $[M + Na]^+$, 630.2462; found 630.2463.

*1-(1-(3-(Benzyloxy)-2-methoxyphenanthro[3,2-d][1,3]dioxol-6-yl)-6,7-dimethoxy-3,4-dihydroisoquinolin-2(1H)-yl)ethanone (**21l**).* White solid, 228 mg, yield: 96%. ^{1}H NMR (400 MHz, $CDCl_3$) δ 8.21 (s, 1H), 7.93 (s, 1H), 7.79 (s, 1H), 7.51–7.49 (m, 2H), 7.42–7.32 (m, 4H), 7.07 (s, 1H), 6.84 (s, 1H), 6.74 (s, 1H), 6.57 (s, 1H), 6.14–6.11 (d, J = 7.44 Hz, 2H), 5.22 (s, 2H), 4.10 (s, 3H), 3.97 (s, 3H), 3.74 (s, 3H), 3.68–3.63 (m, 1H), 3.54–3.46 (s, 1H), 3.12–3.03 (s, 1H), 2.86–2.80 (m, 1H), 2.22 (s, 3H). ^{13}C NMR (100 MHz, $CDCl_3$) δ 169.15, 150.07, 148.21(×2), 147.81, 147.70, 147.65, 136.73, 134.41, 128.58(×2), 128.07, 127.93(×2), 127.42 (×2), 126.85, 126.42(×2), 125.22, 125.07, 111.52, 111.23, 110.37, 103.42, 103.16, 101.37, 100.37, 70.70, 56.12, 55.95, 55.86, 52.92, 39.60, 28.31, 21.67. HRMS calcd for $C_{36}H_{33}NO_7Na$, $[M + Na]^+$, 614.2149; found 614.2141.

*1-(6,7-Dimethoxy-1-(2-methoxyphenanthro[2,3-d][1,3]dioxol-5-yl)-3,4-dihydroisoquinolin-2(1H)-yl)ethanone (**21m**).* White solid, 187 mg, yield: 89%. ^{1}H NMR (400 MHz, $CDCl_3$) δ 8.65–8.63 (d, J = 9.16 Hz, 1H), 7.91 (s, 1H), 7.86–7.85 (d, J = 2.44 Hz, 1H), 7.48 (s, 1H), 7.33–7.30 (m, 1H), 6.98 (s, 1H), 6.78 (s, 1H), 6.71 (s, 1H), 6.55 (s, 1H), 6.07–6.06 (s, 2H), 4.01 (s, 3H), 3.94 (s, 3H), 3.72 (s, 3H), 3.66–3.61 (m, 1H), 3.53–3.45 (m, 1H), 3.09–3.01 (m, 1H), 2.84–2.79 (m, 1H), 2.20 (s, 3H). ^{13}C NMR (100 MHz, $CDCl_3$) δ 169.69, 158.25, 148.41, 148.27, 147.81, 147.67, 134.40, 131.96, 127.87, 127.64, 127.54, 126.91, 126.14, 125.93, 124.91, 116.33, 111.38, 111.20, 106.06, 104.31, 101.37, 100.73, 55.96, 55.87, 55.47, 53.02, 39.79, 28.34, 21.13. HRMS calcd for $C_{29}H_{27}NO_6Na$, $[M + Na]^+$, 508.1731; found 508.1724.

*1-(1-(2,3-Dimethoxyphenanthro[2,3-d][1,3]dioxol-5-yl)-6,7-dimethoxy-3,4-dihydroisoquinolin-2(1H)-yl)ethanone (**21n**).* White solid, 201 mg, yield: 90%. ^{1}H NMR (400 MHz, $CDCl_3$) δ 8.19 (s, 1H), 7.84 (s, 1H), 7.80 (s, 1H), 7.45 (s, 1H), 6.97 (s, 1H), 6.81 (s, 1H), 6.72 (s, 1H), 6.58 (s, 1H), 6.06–6.05 (m, 2H), 4.11 (s, 6H), 3.94 (s, 3H), 3.73 (s, 3H), 3.67–3.61 (m, 1H), 3.51–3.43 (m, 1H), 3.11–3.02 (m, 1H), 2.84–2.79 (m, 1H), 2.19 (s, 3H). ^{13}C NMR (100 MHz, $CDCl_3$) δ 169.11, 149.29, 149.12, 148.32, 148.27, 147.73, 146.84, 134.00, 128.20, 127.86, 126.46, 126.44, 125.94, 125.61, 125.18, 111.53, 111.29, 105.98(×2), 103.12, 101.22, 100.07, 56.64, 55.94(×2), 55.86, 52.75, 39.65, 28.34, 21.45 HRMS calcd for $C_{30}H_{29}NO_7Na$, $[M + Na]^+$, 538.1836; found 538.1829.

*1-(1-(3-Isopropoxy-6,7-dimethoxyphenanthren-9-yl)-6,7-dimethoxy-3,4-dihydroisoquinolin-2(1H)-yl)ethanone (**21o**).* White solid, 196 mg, yield: 92%. ^{1}H NMR (400 MHz, $CDCl_3$) δ 8.20 (s, 1H), 7.92 (s, 1H), 7.90–7.89 (d, J = 2.12 Hz, 1H), 7.57–7.55 (d, J = 8.80 Hz, 1H), 7.44 (s, 1H), 7.14–7.11 (dd, J = 8.76, 2.28 Hz, 1H), 6.87 (s, 1H), 6.73 (s, 1H), 6.59 (s, 1H), 4.81–4.75 (m, 1H), 4.11 (s, 6H), 3.95 (s, 3H), 3.74 (s, 3H), 3.66–3.61 (m, 1H), 3.53–3.45 (m, 1H), 3.11–2.92 (m, 1H), 2.84–2.79 (m, 1H), 2.20 (s, 3H), 1.44–1.42 (dd, J = 6.00, 0.76 Hz, 6H). ^{13}C NMR (100 MHz, $CDCl_3$) δ 169.10, 156.71, 149.80, 148.86, 147.01, 146.28, 133.16, 131.17, 130.38(×2), 129.00, 128.41, 127.61, 126.55, 124.96, 124.58, 116.12, 108.88, 108.35, 107.35, 106.09, 103.60, 100.98, 70.41, 56.67, 56.01, 53.02, 39.46, 28.85, 22.17(×2), 21.46. HRMS calcd for $C_{32}H_{35}NO_6Na$, $[M + Na]^+$, 552.2357; found 552.2369.

*1-(5-(3,6,7-Trimethoxyphenanthren-9-yl)-7,8-dihydro-[1,3]-dioxolo[4,5-g]isoquinolin-6(5H)-yl)ethanone (**22a**).* White solid, 204 mg, yield: 96%. ^{1}H NMR (400 MHz, $CDCl_3$) δ 8.17 (s, 1H), 7.92 (s, 1H), 7.84–7.83 (d, J = 2.20 Hz, 1H), 7.62 (s, 1H), 7.60–7.58 (d, J = 8.76 Hz, 1H), 7.41 (s, 1H), 7.14–7.11 (dd, J = 8.72, 2.36 Hz, 1H), 6.92 (s, 1H), 6.70 (s, 1H), 6.56 (s, 1H), 5.99–5.98 (d, J = 1.08 Hz, 1H), 5.94–5.93 (d, J = 1.12 Hz, 1H), 4.12 (s, 1H), 4.11 (s, 1H), 4.01 (s, 1H), 3.63–3.60 (m, 1H), 3.49–3.42 (m, 1H), 3.07–2.98 (m, 1H), 2.81–2.76 (m, 1H), 2.18 (s, 1H). ^{13}C NMR (100 MHz, $CDCl_3$) δ 169.04, 158.59, 149.90, 148.93, 147.04, 146.31, 133.21, 131.06, 130.47, 129.03, 128.41,

127.65, 126.69, 125.02, 124.63, 115.24, 108.89, 108.37, 106.20, 103.84, 103.64, 100.98, 56.68, 56.04, 55.58, 53.02, 39.47, 28.86, 21.48. HRMS calcd for $C_{29}H_{27}NO_6Na$, $[M + Na]^+$, 508.1731; found 508.1736.

*1-(5-(2-Methoxyphenanthro[3,2-d][1,3]dioxol-6-yl)-7,8-dihydro-[1,3]dioxolo[4,5-g]isoquinolin-6(5H)-yl)ethanone (**22b**).* White solid, 213 mg, yield: 95%. ^{1}H NMR (600 MHz, $CDCl_3$) δ 8.18 (s, 1H), 7.89 (s, 1H), 7.79–7.78 (d, J = 2.16 Hz, 1H), 7.59–7.57 (d, J = 8.76 Hz, 1H), 7.34 (s, 1H), 7.14–7.11 (dd, J = 8.70, 2.28 Hz, 1H), 6.94 (s, 1H), 6.70 (s, 1H), 6.52 (s, 1H), 6.14–6.12 (d, J = 11.46 Hz, 2H), 5.99 (s, 1H), 5.95–5.94 (d, J = 1.14 Hz, 1H), 4.01 (s, 3H), 3.64–3.61 (m, 1H), 3.50–3.45 (m, 1H), 3.06–3.00 (m, 1H), 2.81–2.78 (m, 1H), 2.20 (s, 3H). ^{13}C NMR (150 MHz, $CDCl_3$) δ 160.11, 158.59, 148.41, 147.71, 146.99, 146.29, 133.66, 131.31, 130.33, 129.05, 128.51, 127.99, 127.59, 126.36, 124.98, 116.26, 108.79, 108.33, 103.44, 103.16, 101.45, 100.97, 100.89, 55.46, 53.09, 39.41, 21.66, 28.80. HRMS calcd for $C_{28}H_{24}NO_6$ $[M + H]^+$, 470.1598; found 470.1615.

*1-(5-(2,3,6-Trimethoxyphenanthren-9-yl)-7,8-dihydro-[1,3]-dioxolo[4,5-g]isoquinolin-6(5H)-yl)ethanone (**22c**).* White solid, 203 mg, yield: 95%. ^{1}H NMR (400 MHz, $CDCl_3$) δ 8.64–8.61 (d, J = 9.16 Hz, 1H), 7.92–7.91 (d, J = 2.44 Hz, 1H), 7.86 (s, 1H), 7.46 (s, 1H), 7.32–7.29 (m, 1H), 7.02 (s, 1H), 6.84 (s, 1H), 6.71 (s, 1H), 6.55 (s, 1H), 5.99 (s, 1H), 5.92 (s, 1H), 4.10 (s, 3H), 4.02 (s, 3H), 3.98 (s, 3H), 3.63–3.58 (m, 1H), 3.51–3.43 (m, 1H), 3.07–2.98 (m, 1H), 2.82–2.76 (m, 1H), 2.18 (s, 3H). ^{13}C NMR (100 MHz, $CDCl_3$) δ 169.10, 158.14, 149.40, 149.39, 147.00, 146.30, 134.65, 131.67, 129.07, 127.62, 127.29, 127.15, 126.32, 124.93, 124.25, 115.21, 108.87, 108.67, 108.32, 104.83, 103.25, 100.98, 56.08, 55.94, 55.55, 52.85, 39.48, 28.85, 21.57. HRMS calcd for $C_{29}H_{27}NO_6Na$, $[M + Na]^+$, 508.1731; found 508.1726.

*1-(5-(2,3,6,7-Tetramethoxyphenanthren-9-yl)-7,8-dihydro-[1,3]-dioxolo[4,5-g]isoquinolin-6(5H)-yl)ethanone (**22d**).* White solid, 229 mg, yield: 97%. ^{1}H NMR (400 MHz, $CDCl_3$) δ 8.17 (s, 1H), 7.85 (s, 1H), 7.79 (s, 1H), 7.45 (s, 1H), 7.04 (s, 1H), 6.91 (s, 1H), 6.75 (s, 1H), 6.60 (s, 1H), 6.03–6.02 (d, J = 0.76 Hz, 1H), 5.97 (s, 1H), 4.16 (s, 3H), 4.14 (s, 3H), 4.13 (s, 3H), 4.00 (s, 3H), 3.67–3.62 (m, 1H), 3.53–3.47 (m, 1H), 3.12–3.05 (m, H), 2.86–2.82 (m, 1H), 2.24 (s, 3H). ^{13}C NMR (100 MHz, $CDCl_3$) δ 169.08, 149.59, 149.19, 149.10, 148.77, 147.04, 146.33, 133.80, 129.10, 127.83, 127.64, 125.52, 125.23, 124.80, 124.43, 108.94, 108.73, 108.37, 106.11, 103.10, 102.70, 101.01, 56.66, 56.13, 56.08, 55.93, 53.10, 39.51, 28.91, 21.47. HRMS calcd for $C_{30}H_{29}NO_7Na$, $[M + Na]^+$, 538.1836; found 538.1835.

*1-(5-(2,3,5,6,7-Pentamethoxyphenanthren-9-yl)-7,8-dihydro-[1,3]-dioxolo[4,5-g]isoquinolin-6(5H)-yl)ethanone (**22e**).* White solid, 221 mg, yield: 90%. ^{1}H NMR (400 MHz, $CDCl_3$) δ 9.09 (s, 1H), 8.02 (s, 1H), 7.39 (s, 1H), 6.99 (s, 1H), 6.90 (s, 1H), 6.71 (s, 1H), 6.55 (s, 1H), 6.00–5.99 (d, J = 0.90 Hz, 1H), 5.93–5.92 (d, J = 0.96 Hz, 1H), 4.08 (s, 6H), 4.05 (s, 3H), 4.00 (s, 3H), 3.97 (s, 3H), 3.90 (s, 3H), 3.61–3.60 (m, 1H), 3.48–3.42 (m, 1H), 3.06–3.00 (m, 1H), 2.81–2.78 (m, 1H), 2.19 (s, 3H). ^{13}C-NMR (400 MHz, $CDCl_3$) δ 169.08, 152.14, 151.52, 148.99, 147.94, 146.96, 146.26, 142.42, 133.40, 130.01, 129.10, 128.22, 127.58, 125.74, 124.32, 119.07, 108.84, 108.34(×2), 107.42, 102.59, 100.95, 61.26, 60.49, 56.60, 55.77, 55.71, 53.05, 39.45, 28.77, 21.47. HRMS calcd for $C_{39}H_{41}NO_9Na$, $[M + Na]^+$, 568.2111; found 568.2109.

*1-(5-(2,3-Dimethoxyphenanthro[3,2-d][1,3]dioxol-6-yl)-7,8-dihydro-[1,3]dioxolo[4,5-g]isoquinolin-6(5H)-yl)ethanone (**22f**).* White solid, 179 mg, yield: 86%. ^{1}H NMR (400 MHz, $CDCl_3$) δ 8.14 (s, 1H), 7.89 (s, 1H), 7.73 (s, 1H), 7.34 (s, 1H), 6.99 (s, 1H), 6.89 (s, 1H), 6.70 (s, 1H), 6.52 (s, 1H), 6.11–6.09 (d, J = 6.80 Hz, 1H), 5.98 (s, 1H), 5.93–5.92 (d, J = 1.00 Hz, 1H), 4.08 (s, 3H), 3.97 (s, 3H), 3.64–3.59 (m, 1H), 3.50–3.43 (m, 1H), 3.07–2.98 (m, 1H), 2.82–2.77 (m, 1H), 2.19 (s, 3H). ^{13}C NMR(100 MHz, $CDCl_3$) δ 169.19, 149.61, 148.89, 147.85, 147.68, 147.02, 146.34, 134.23, 129.14, 127.86, 127.57, 126.51, 125.23, 124.84, 108.84, 108.43, 108.32, 103.32, 102.74, 101.38, 100.99, 100.35, 56.00, 55.92, 53.22, 39.46, 28.83, 21.55. HRMS calcd for $C_{29}H_{26}NO_7$, $[M + H]^+$, 500.1704; found 500.1703.

*1-(5-(3-(Benzyloxy)-2,6-dimethoxyphenanthren-9-yl)-7,8-dihydro-[1,3]dioxolo[4,5-g]isoquinolin-6(5H)-yl)ethanone (**22g**).* White solid, 251 mg, yield: 88%. ^{1}H NMR (400 MHz, $CDCl_3$) δ 8.59–8.57 (d, J = 9.20 Hz, 1H), 7.89 (s, 1H), 7.71–7.70 (d, J = 2.40 Hz, 1H), 7.43–7.37 (m, 3H), 7.33–7.28 (m, 2H), 7.03 (s, 1H), 6.83 (s, 1H), 6.70 (s, 1H), 6.53 (s, 1H), 5.98 (s, 1H), 5.92–5.91 (d, J = 1.12 Hz, 1H), 5.37 (s, 2H), 3.98 (s, 3H), 3.97 (s, 3H), 3.61–3.56 (m, 1H), 3.49–3.41 (m, 1H), 3.06–2.97 (m, 1H), 2.80–2.75 (m, 1H), 2.17 (s, 3H). ^{13}C NMR (100 MHz, $CDCl_3$) δ 169.03, 158.14, 150.07, 148.48, 147.00, 146.31, 137.07, 134.87, 131.64, 129.11, 128.69 (×2), 128.04, 127.64, 127.38(×2), 127.18, 127.09, 126.64, 124.85, 124.13, 115.73, 108.96, 108.87, 108.33, 106.56, 104.22, 100.97, 71.49, 55.98, 55.41, 52.81, 39.46, 28.86, 21.59. HRMS calcd for $C_{35}H_{31}NO_6Na$, $[M + Na]^+$, 584.2044; found 584.2022.

*1-(5-(3-(Benzyloxy)-2,6,7-trimethoxyphenanthren-9-yl)-7,8-dihydro-[1,3]dioxolo[4,5-g]isoquinolin-6(5H)-yl)ethanone (**22h**).* White solid, 258 mg, yield: 91%. ^{1}H NMR (400 MHz, $CDCl_3$) δ 8.12 (s, 1H), 7.78 (s, 1H), 7.59 (s, 1H), 7.57 (s, 1H), 7.55 (s, 1H), 7.41–7.40 (d, J = 1.28 Hz, 1H), 7.39 (s, 1H), 7.37 (s, 1H), 7.33–7.30 (m, 1H), 7.02 (s, 1H), 6.86 (s, 1H), 6.71 (s, 1H), 6.55 (s, 1H), 6.00–5.99 (d, J = 0.96 Hz, 1H), 5.93–5.92 (d, J = 1.08 Hz, 1H), 5.39 (s, 2H), 4.08 (s, 3H), 4.06 (s, 3H), 3.98 (s, 3H), 3.62–3.57 (m, 1H), 3.47–3.40 (m, 1H), 3.07–2.98 (m, 1H), 2.81–2.76 (m, 1H), 2.17 (s, 3H). ^{13}C NMR (100 MHz, $CDCl_3$) δ 169.14, 149.32, 149.09, 149.01, 148.55, 147.05, 146.33, 137.25, 133.87, 129.00, 128.70(×2), 128.04, 127.72, 127.58, 127.30(×2), 125.47, 125.29, 124.75, 124.25, 108.91, 108.35, 106.23, 105.94, 102.91, 101.01, 71.68, 56.64, 55.97, 55.85, 53.13, 39.50, 28.88, 21.33. HRMS calcd for $C_{36}H_{33}NO_7Na$, $[M + Na]^+$, 614.2149; found 614.2160.

*1-(5-(2-(Benzyloxy)-3-methoxyphenanthro[3,2-d][1,3]dioxol-6-yl)-7,8-dihydro-[1,3]dioxolo[4,5-g]isoquinolin-6(5H)-yl)ethanone (**22i**).* White solid, 230 mg, yield: 90%. ^{1}H NMR (400 MHz, $CDCl_3$) δ 8.30 (s, 1H), 8.12 (s, 1H), 8.03 (s, 1H), 7.55 (s, 1H), 7.53 (s, 1H), 7.43–7.40 (m, 2H), 7.36–7.32 (m, 1H), 7.19 (s, 1H), 7.17 (s, 1H), 6.92 (s, 1H), 6.85 (s, 1H), 6.64 (s, 1H), 6.19 (s, 1H), 6.16 (s, 1H), 6.03 (s, 1H), 5.97 (s, 1H), 5.35 (s, 2H), 3.84 (s, 3H), 3.72–3.67 (m, 1H), 3.29–3.21 (m, 1H), 3.04–2.95 (m, 1H), 2.79–2.74 (m, 1H), 2.12 (s, 3H). ^{13}C NMR (100 MHz, $CDCl_3$) δ 169.06, 149.45, 148.63, 147.79, 147.61, 146.99, 146.31, 136.84, 134.46, 129.17, 128.67(×2), 128.03, 127.80, 127.62, 127.40(×2),

126.67, 126.49, 125.53, 124.69, 108.83, 108.74, 108.32, 105.64, 103.33, 101.31, 100.97, 100.33, 71.17, 55.97, 53.10, 39.42, 28.82, 21.62. HRMS calcd for $C_{36}H_{33}NO_7Na$, $[M + Na]^+$, 598.1836; found 598.1854.

*1-(5-(2-(Benzyloxy)-3,6-dimethoxyphenanthren-9-yl)-7,8-dihydro-[1,3]dioxolo[4,5-g]isoquinolin-6(5H)-yl)ethanone (**22j**).* White solid, 229 mg, yield: 89%. ^{1}H-NMR (400 MHz, $CDCl_3$) δ 8.64–8.61 (d, J = 9.20 Hz, 1H), 7.93–7.92 (d, J = 2.48 Hz, 1H), 7.89 (s, 1H), 7.49–7.45 (m, 3H), 7.41–7.37 (m, 2H), 7.34–7.29 (m, 2H), 7.11 (s, 1H), 6.82 (s, 1H), 6.70 (s, 1H), 6.54 (s, 1H), 5.99–5.98 (d, J = 0.88 Hz, 2H), 5.93–5.92 (d, J = 1.24 Hz, 2H), 5.21 (s, 2H), 4.09 (s, 3H), 4.03 (s, 3H), 3.63–3.57 (m, 1H), 3.51–3.43 (m, 1H), 3.06–2.97 (m, 1H), 2.81–2.76 (m, 1H), 2.17 (s, 3H). ^{13}C NMR (100 MHz, $CDCl_3$) δ 169.03, 158.15, 149.92, 148.90, 146.98, 146.29, 136.73, 134.72, 131.66, 129.12, 128.58(×2), 127.96, 127.64, 127.45(×2), 127.23(×2), 126.34, 125.03, 124.59, 115.26, 110.68, 108.89, 108.34, 104.89, 103.93, 100.95, 70.79, 56.25, 55.55, 52.80, 39.48, 28.85, 21.62. HRMS calcd for $C_{36}H_{35}NO_6Na$, $[M + Na]^+$, 584.2225; found 584.2229.

*1-(5-(2-(Benzyloxy)-3,6,7-trimethoxyphenanthren-9-yl)-7,8-dihydro-[1,3]dioxolo[4,5-g]isoquinolin-6(5H)-yl)ethanone (**22k**).* White solid, 201 mg, yield: 92%. ^{1}H NMR (400 MHz, $CDCl_3$) δ 8.16 (s, 1H), 7.84 (s, 1H), 7.80 (s, 1H), 7.42 (s, 1H), 7.39–7.37 (m, 2H), 7.34–7.30 (m, 1H), 7.11 (s, 1H), 6.86 (s, 1H), 6.71 (s, 1H), 6.56 (s, 1H), 5.99 (s, 1H), 5.93–5.92 (d, J = 0.84 Hz, 1H), 5.20 (s, 2H), 4.13 (s, 3H), 4.10 (s, 6H), 3.63–3.58 (m, 1H), 3.50–3.42 (m, 1H), 3.08–2.99 (m, 1H), 2.82–2.77 (m, 1H), 2.19 (s, 3H). ^{13}C NMR (100 MHz, $CDCl_3$) δ 169.03, 150.09, 149.21, 149.08, 148.20, 147.01, 146.30, 136.80, 133.86, 129.09, 128.57(×2), 127.95, 127.79, 127.67, 127.46(×2), 125.61, 125.25, 124.76, 110.76, 108.93, 108.39, 106.15, 103.38, 103.16, 100.98, 70.80, 56.63, 56.32, 56.07, 53.04, 39.49, 28.86, 21.47. HRMS calcd for $C_{36}H_{33}NO_7Na$, $[M + Na]^+$, 614.2149; found 614.2149.

*1-(5-(3-(Benzyloxy)-2-methoxyphenanthro[3,2-d][1,3]dioxol-6-yl)-7,8-dihydro-[1,3]dioxolo[4,5-g]isoquinolin-6(5H)-yl)ethanone (**22l**).* White solid, 222 mg, yield: 94%. ^{1}H NMR (400 MHz, $CDCl_3$) δ 8.14 (s, 1H), 7.90 (s, 1H), 7.76 (s, 1H), 7.49 (s, 1H), 7.47 (s, 1H), 7.40–7.36 (m, 2H), 7.33–7.30 (m, 2H), 7.08 (s, 1H), 6.86 (s, 1H), 6.69 (s, 1H), 6.50 (s, 1H), 6.11 (s, 1H), 6.09 (s, 1H), 5.98 (s, 1H), 5.92–5.91 (d, J = 0.96 Hz, 1H), 5.20 (s, 2H), 4.07 (s, 3H), 3.63–3.58 (m, 1H), 3.49–3.43 (m, 1H), 3.06–2.97 (m, 1H), 2.81–2.76 (m, 1H), 2.19 (s, 3H). ^{13}C NMR (100 MHz, $CDCl_3$) δ 169.08, 150.11, 148.26, 147.82, 147.70, 146.98, 146.31, 136.77, 134.32, 129.16, 128.57(×2), 127.94, 127.83, 127.61, 127.44(×2), 126.82, 126.47, 125.20, 125.15, 110.44, 108.85, 108.35, 103.38, 103.24, 101.37, 100.96, 100.39, 70.79, 56.11, 53.14, 39.44, 28.82, 21.64. HRMS calcd for $C_{35}H_{29}NO_7Na$, $[M + Na]^+$, 598.1836; found 598.1854.

*1-(5-(2-Methoxyphenanthro[2,3-d][1,3]dioxol-5-yl)-7,8-dihydro-[1,3]dioxolo[4,5-g]isoquinolin-6(5H)-yl)ethanone (**22m**).* White solid, 184 mg, yield: 88%. ^{1}H NMR (400 MHz, $CDCl_3$) δ 8.61–8.59 (d, J = 9.16 Hz, 1H), 7.90 (s, 1H), 7.85–7.84 (d, J = 2.48 Hz, 1H), 7.44 (s, 1H), 7.31–7.26 (m, 1H), 7.30–7.28 (m, 1H), 7.00 (s, 1H), 6.81 (s, 1H), 6.68 (s, 1H), 6.52 (s, 1H), 6.06 (s, 2H), 5.97 (s, 1H), 5.93–5.92 (d, J = 1.20 Hz, 1H), 4.00 (s, 3H), 3.63–3.57 (m, 1H), 3.49–3.41 (m, 1H), 3.05–3.00 (m, 1H), 2.80–2.75 (m, 1H), 2.17 (s, 3H). ^{13}C NMR (100 MHz, $CDCl_3$) δ 169.13, 158.19, 148.17, 147.61, 147.03, 146.32, 134.76, 131.96, 128.91, 127.64(×2), 127.57, 127.05, 125.88, 124.99, 116.25, 108.77, 108.34, 106.00, 104.21, 101.33, 100.98, 100.75, 55.44, 52.79, 39.50, 28.84, 21.53. HRMS calcd for $C_{28}H_{23}NO_6Na$, $[M + Na]^+$, 492.1418; found 492.1389.

*1-(5-(2,3-Dimethoxyphenanthro[2,3-d][1,3]dioxol-5-yl)-7,8-dihydro-[1,3]dioxolo[4,5-g]isoquinolin-6(5H)-yl)ethanone (**22n**).* White solid, 197 mg, yield: 89%. ^{1}H NMR (400 MHz, $CDCl_3$) δ 8.15 (s, 1H), 7.83 (s, 1H), 7.79 (s, 1H), 7.41 (s, 1H), 7.00 (s, 1H), 6.84 (s, 1H), 6.69 (s, 1H), 6.55 (s, 1H), 6.05 (s, 2H), 5.98–5.97 (d, J = 1.24 Hz, 1H), 5.93–5.92 (d, J = 1.28 Hz, 1H), 4.10 (s, 3H), 4.09 (s, 3H), 3.63–3.58 (m, 1H), 3.48–3.40 (m, 1H), 3.07–2.98 (m, 1H), 2.80–2.75 (m, 1H), 2.17 (s, 3H). ^{13}C NMR (100 MHz, $CDCl_3$) δ 169.01, 149.26, 149.10, 148.25, 147.04, 146.82, 146.31, 133.92, 128.95, 128.16, 127.62, 126.40, 125.97, 125.56, 125.21, 108.37, 105.95(×2), 103.12, 108.82, 101.22, 100.98, 100.10, 56.63, 55.92, 52.97, 39.49, 28.85, 21.44. HRMS calcd for $C_{29}H_{26}NO_7$, $[M + H]^+$, 500.1704; found 500.1703.

*1-(5-(3-Isopropoxy-6,7-dimethoxyphenanthren-9-yl)-7,8-dihydro-[1,3]dioxolo[4,5-g]isoquinolin-6(5H)-yl)ethanone (**22o**).* White solid, 193 mg, yield: 92%. ^{1}H NMR (400 MHz, $CDCl_3$) δ 8.16 (s, 1H), 7.92 (s, 1H), 7.89–7.88 (d, J = 1.88 Hz, 1H), 7.59–7.57 (d, J = 8.76 Hz, 1H), 7.40 (s, 1H), 7.13–7.10 (dd, J = 8.72, 2.28 Hz, 1H), 6.90 (s, 1H), 6.70 (s, 1H), 6.56 (s, 1H), 5.98–5.93 (m, 2H), 4.81–4.75 (m, 1H), 4.11 (s, 3H), 4.10 (s, 3H), 3.63–3.58 (m, 1H), 3.50–3.43 (m, 1H), 3.07–2.98 (m, 1H), 2.81–2.76 (m, 1H), 2.18 (s, 3H), 1.44–1.42 (dd, J = 6.00, 1.36 Hz, 6H). ^{13}C NMR (100 MHz, $CDCl_3$) δ 169.12, 156.73, 149.83, 148.88, 147.02, 146.29, 133.16, 131.18, 130.38, 129.01, 128.41, 127.62, 126.57, 124.97, 124.59, 116.16, 108.87, 108.35, 107.36, 106.12, 103.65, 100.97, 70.43, 56.66, 56.02, 53.03, 39.46, 28.85, 22.18(×2), 21.45. HRMS calcd for $C_{31}H_{31}NO_6Na$, $[M + Na]^+$, 536.2044; found 536.2048.

General synthetic procedure for the preparation of 21p–u and 22p–u. To a solution of **21g–l** or **22g–l** (0.17 mmol) in absolution MeOH (30 mL) was added 1,4-cyclohexadiene (3.5 mL) and Pd/C (10%, 50 mg) in an ultrasonic reactor for 100 min at 25 °C. The solution was filtered and dried under reduced pressure to give off-white solids which were purified by recrystallization with MeOH to furnish **21p–u** or **22p–u** as white solids. For example:

*1-(1-(3-Hydroxy-2,6-dimethoxyphenanthren-9-yl)-6,7-dimethoxy-3,4-dihydroisoquinolin-2(1H)-yl)ethanone (**21p**).* White solid, 87 mg, yield: 97%. ^{1}H NMR (400 MHz, DMSO-d_6) δ 9.44 (s, 1H), 8.50–8.48 (d, J = 9.24 Hz, 1H), 8.01 (s, 1H), 7.90–7.88 (d, J = 2.20 Hz, 1H), 7.29 (s, 1H), 7.22–7.19 (dd, J = 9.12, 2.24 Hz, 1H), 7.14 (s, 1H), 6.86 (s, 1H), 6.82 (s, 1H), 6.65 (s, 1H), 3.97 (s, 3H), 3.87 (s, 3H), 3.80 (s, 1H), 3.73–3.68 (m, 1H), 3.59 (s, 1H), 3.32–3.24 (m, 1H), 3.05–2.96 (s, 1H), 2.81–2.76 (m, 1H), 2.11 (s, 3H). ^{13}C NMR (100 MHz, DMSO-d_6) δ 169.09, 158.18, 149.26, 148.35, 147.63, 147.54, 134.10, 131.57, 128.06, 127.41, 127.21, 126.94, 125.73, 124.87, 124.49, 116.16, 112.28, 112.00, 109.33, 107.74, 104.31, 56.05, 55.89(×2), 55.88, 55.76, 52.24, 28.16, 21.85. HRMS calcd for $C_{29}H_{30}NO_6$, $[M + H]^+$, 488.2068; found 488.2066.

*1-(1-(3-Hydroxy-2,6,7-trimethoxyphenanthren-9-yl)-6,7-dimethoxy-3,4-dihydroisoquinolin-2(1H)-yl)ethanone (**21q**).* White solid, 84 mg, yield: 96%. ^{1}H NMR (400 MHz, DMSO-d_6) δ 9.33 (s, 1H), 8.06 (s, 1H), 7.94 (s, 1H), 7.85 (s, 1H), 7.27 (s, 1H), 7.09 (s, 1H), 6.86 (s, 1H), 6.81 (s, 1H), 6.66 (s, 1H), 3.98 (s, 3H), 3.89 (s, 3H), 3.85 (s, 3H), 3.81 (s, 3H), 3.73–3.68 (m, 1H), 3.60 (s, 3H), 3.28–3.21 (m, 1H), 3.05–2.97 (m, 1H), 2.80–2.75 (m, 1H), 2.13 (s, 3H). ^{13}C NMR (100 MHz, DMSO-d_6) δ 168.79, 148.67, 148.47, 147.96, 147.88, 147.13, 147.09, 127.52, 132.82, 127.05, 126.93, 124.72, 124.26, 124.21, 124.12, 111.83, 111.59, 108.75, 106.76, 105.87, 103.53, 55.62, 55.52, 55.42, 55.40, 52.03, 27.72, 21.20. HRMS calcd for $C_{30}H_{32}NO_7$, $[M + H]^+$, 518.2173; found 518.2184.

*1-(1-(2-Hydroxy-3-methoxyphenanthro[3,2-d][1,3]dioxol-6-yl)-6,7-dimethoxy-3,4-dihydroisoquinolin-2(1H)-yl)ethanone (**21r**).* White solid, 79 mg, yield: 95%. ^{1}H NMR (400 MHz, DMSO-d_6) δ 9.39 (s, 1H), 8.05 (s, 1H), 7.96 (s, 1H), 7.86 (s, 1H), 7.18 (s, 1H), 7.10 (s, 1H), 6.86 (s, 2H), 6.64 (s, 1H), 6.18 (s, 1H), 6.14 (s, 1H), 3.85 (s, 3H), 3.81 (s, 3H), 3.73–3.68 (m, 1H), 3.59 (s, 3H), 3.31–3.24 (m, 1H), 3.06–2.97 (m, 1H), 2.81–2.76 (m, 1H), 2.12 (s, 3H). ^{13}C NMR (100 MHz, DMSO-d_6) δ 169.25, 148.72, 148.40, 147.75, 147.73, 147.68, 147.45, 133.72, 128.07, 127.96, 127.38, 126.58, 126.29, 125.18, 124.75, 112.30, 112.04, 109.08, 107.25, 103.02, 101.71, 101.11, 56.04(×2), 55.89(×2), 52.63, 28.12, 21.88. HRMS calcd for $C_{29}H_{28}NO_7$, $[M + H]^+$, 502.1860; found 502.1847.

*1-(1-(2-Hydroxy-3,6-dimethoxyphenanthren-9-yl)-6,7-dimethoxy-3,4-dihydroisoquinolin-2(1H)-yl)ethanone (**21s**).* White solid, 75 mg, yield: 92%. ^{1}H NMR (400 MHz, DMSO-d_6) δ 9.48 (s, 1H), 8.50–8.48 (d, J = 9.24 Hz, 1H), 8.09–8.08 (d, J = 2.36 Hz, 1H), 8.04 (s, 1H), 7.28 (s, 1H), 7.23–7.20 (m, 1H), 6.91 (s, 1H), 6.85 (s, 1H), 6.64 (s, 2H), 4.02–3.99 (d, J = 12.72 Hz, 6H), 3.81 (s, 3H), 3.73–3.68 (s, 1H), 3.59 (s, 3H), 3.28–3.23 (m, 1H), 3.04–2.95 (m, 1H), 2.82–2.76 (m, 1H), 2.11 (s, 3H). ^{13}C NMR (100 MHz, DMSO-d_6) δ 168.95, 158.27, 149.24, 148.39, 147.78, 147.67, 134.74, 132.08, 128.07, 127.34, 126.93, 126.71, 124.63, 123.43, 115.40, 112.46, 112.27, 111.96, 105.00, 104.58, 56.57, 56.38, 55.92, 55.85, 52.26, 31.06, 28.15, 21.83, 18.95. HRMS calcd for $C_{29}H_{30}NO_6$, $[M + H]^+$, 488.2068; found 488.2075.

*1-(1-(2-Hydroxy-3,6,7-trimethoxyphenanthren-9-yl)-6,7-dimethoxy-3,4-dihydroisoquinolin-2(1H)-yl)ethanone (**21t**).* White solid, 79 mg, yield: 93%. ^{1}H NMR (400 MHz, DMSO-d_6) δ 9.33 (s, 1H), 8.06 (s, 1H), 8.01 (s, 1H), 7.97 (s, 1H), 7.27 (s, 1H), 6.88 (s, 1H), 6.86 (s, 1H), 6.66 (s, 1H), 6.65 (s, 1H), 4.03 (s, 6H), 3.90 (s, 3H), 3.81 (s, 3H), 3.73–3.68 (m, 1H), 3.60 (s, 1H), 3.28–3.20 (m, 1H), 3.05–2.96 (m, 1H), 2.81–2.76 (m, 1H), 2.13 (s, 3H). ^{13}C NMR (100 MHz, DMSO-d_6) δ 169.32, 149.46, 149.30, 148.86, 148.40, 147.64, 146.96, 134.05, 128.00, 127.46, 127.02, 125.56, 125.28, 125.01, 123.71, 112.37(×2), 112.08, 106.42, 104.54, 104.28, 56.48, 56.40, 56.09, 55.94(×2), 55.37, 52.51, 28.16, 21.71. HRMS calcd for $C_{30}H_{32}NO_7$, $[M + H]^+$, 518.2173; found 518.2177.

*1-(1-(3-Hydroxy-2-methoxyphenanthro[3,2-d][1,3]dioxol-6-yl)-6,7-dimethoxy-3,4-dihydroisoquinolin-2(1H)-yl)ethanone (**21u**).* White solid, 80 mg, yield: 91%. ^{1}H NMR (400 MHz, DMSO-d_6) δ 9.38 (s, 1H), 8.30 (s, 1H), 8.04 (s, 1H), 7.97 (s, 1H), 7.18 (s, 1H), 6.89 (s, 1H), 6.85 (s, 1H), 6.69 (s, 1H), 6.63 (s, 1H), 6.19–6.16 (d, J = 13.76 Hz, 2H), 4.00 (s, 3H), 3.81 (s, 3H), 3.73–3.68 (m, 1H), 3.59 (s, 3H), 3.31–3.23 (s, 1H), 3.05–2.96 (s, 1H), 2.82–2.77 (m, 1H), 2.13 (s, 3H). ^{13}C NMR (100 MHz, DMSO-d_6) δ 169.25, 149.57, 148.39, 147.83, 147.65, 147.20, 147.11, 134.37, 128.02, 127.39, 127.33, 126.22, 125.55, 126.97, 124.25, 112.28, 112.03 (×2), 104.28, 102.96, 101.69(×2), 56.40(×2), 55.92(×2), 52.58, 39.60, 28.04, 21.90. HRMS calcd for $C_{29}H_{28}NO_7$, $[M + H]^+$, 524.1680; found 524.1676.

*1-(5-(3-Hydroxy-2,6-dimethoxyphenanthren-9-yl)-7,8-dihydro-[1,3]dioxolo[4,5-g]isoquinolin-6(5H)-yl)ethanone (**22p**).* White solid, 83 mg, yield: 93%. ^{1}H NMR (400 MHz, DMSO-d) δ 9.45 (s, 1H), 8.46–8.44 (d, J = 8.12 Hz, 1H), 8.00 (s, 1H), 7.89–7.88 (d, J = 2.12 Hz, 1H), 7.25 (s, 1H), 7.21–7.20 (d, J = 2.04 Hz, 1H), 7.18 (s, 1H), 6.85 (s, 1H), 6.84 (s, 1H), 6.65 (s, 1H), 6.03 (s, 1H), 5.97 (s, 1H), 3.88 (s, 3H), 3.72–3.67 (m, 1H), 3.30–3.22 (m, 1H), 3.97 (s, 3H), 3.03–2.94 (s, 1H), 2.79–2.74 (m, 1H), 2.09 (s, 3H). ^{13}C NMR (100 MHz, DMSO-d_6) δ 169.11, 158.18, 149.26, 147.55, 146.88, 146.07, 134.01, 131.57, 129.26, 128.76, 127.25, 126.92, 125.68, 124.78, 124.49, 116.16, 109.39, 109.01, 108.73, 107.73, 104.32, 101.25, 56.05, 55.76(×2), 52.47, 28.67, 21.85. HRMS calcd for $C_{28}H_{26}NO_6$, $[M + H]^+$, 472.1755; found 472.1753.

*1-(5-(3-Hydroxy-2,6,7-trimethoxyphenanthren-9-yl)-7,8-dihydro-[1,3]dioxolo[4,5-g]isoquinolin-6(5H)-yl)ethanone (**22q**).* White solid, 83 mg, yield: 97%. ^{1}H NMR (400 MHz, DMSO-d_6) δ 9.35 (s, 1H), 8.03 (s, 1H), 7.94 (s, 1H), 7.86 (s, 1H), 7.25 (s, 1H), 7.14 (s, 1H), 6.86 (s, 1H), 6.84 (s, 1H), 6.68 (s, 1H), 6.05 (s, 1H), 5.99 (s, 1H), 3.99 (s, 3H), 3.89 (s, 3H), 3.87 (s, 3H), 3.73–3.68 (m, 1H), 3.26–3.18 (m, 1H), 3.04–2.96 (m, 1H), 2.79–2.74 (m, 1H), 2.13 (s, 3H). ^{13}C NMR (100 MHz, DMSO-d_6) δ 169.31, 149.18, 148.96, 148.46, 147.61, 146.91, 146.07, 133.22, 129.22, 128.78, 127.62, 125.14, 124.77, 124.74, 124.57, 109.31, 109.03, 108.79, 107.27, 106.37, 104.06, 101.26, 56.12, 56.03(×2), 52.76, 39.26, 28.75, 21.69. HRMS calcd for $C_{29}H_{28}NO_7$, $[M + H]^+$, 502.1860; found 502.1862.

*1-(5-(2-Hydroxy-3-methoxyphenanthro[3,2-d][1,3]dioxol-6-yl)-7,8-dihydro-[1,3]dioxolo[4,5-g]isoquinolin-6(5H)-yl)ethanone (**22r**).* White solid, 75 mg, yield: 90%. ^{1}H NMR (400 MHz, DMSO-d_6) δ 9.39 (s, 1H), 8.00 (s, 1H), 7.95 (s, 1H), 7.85 (s, 1H), 7.14 (s, 2H), 6.86 (s, 1H), 6.85 (s, 1H), 6.63 (s, 1H), 6.17 (s, 1H), 6.14 (s, 1H), 6.03 (s, 1H), 5.97 (s, 1H), 3.86 (s, 3H), 3.72–3.67 (m, 1H), 3.28–3.21 (m, 1H), 3.04–2.95 (m, 1H), 2.79–2.74 (m, 1H), 2.11 (s, 3H). ^{13}C NMR (100 MHz, DMSO-d_6) δ 169.25, 148.71, 147.75, 147.43, 146.91, 146.09, 133.61, 129.25, 128.72, 127.99, 126.48, 126.28, 125.16, 124.69, 109.14, 109.00, 108.72, 107.23, 103.00, 101.71, 101.26, 101.10, 56.05, 52.85, 39.21, 28.64, 21.88. $C_{28}H_{23}NO_7Na$, $[M + Na]^+$, 508.1367; found 508.1353.

*1-(5-(2-Hydroxy-3,6-dimethoxyphenanthren-9-yl)-7,8-dihydro-[1,3]dioxolo[4,5-g]isoquinolin-6(5H)-yl)ethanone (**22s**).* White solid, 71 mg, yield: 87%. ^{1}H NMR (400 MHz, DMSO-d_6) δ 9.47 (s, 1H), 8.46–8.44 (d, J = 9.24 Hz, 1H), 8.09–8.08 (d, J = 2.36 Hz, 1H), 8.04 (s, 1H), 7.24–7.19 (m, 1H), 6.94 (s, 1H), 6.84 (s, 1H), 6.66 (s, 1H), 6.64 (s, 1H), 6.01–5.98 (d, J = 11.68 Hz, 2H), 4.03 (s, 3H), 4.00 (s, 3H), 3.72–3.66 (m, 1H), 3.29–3.21 (m, 1H), 3.02–2.93 (m, 1H), 2.80–2.75 (m, 1H), 2.10 (s, 3H). ^{13}C NMR (100 MHz, DMSO-d_6) δ 169.11, 158.33, 149.33, 147.85, 146.88,

146.07, 134.77, 132.12, 129.24, 128.77, 126.92, 126.66, 124.56, 123.44, 115.50, 112.47, 108.95, 108.66, 105.22, 104.74, 101.25, 56.49, 55.98, 56.45, 52.45, 28.60, 21.85, 19.02. HRMS calcd for $C_{28}H_{26}NO_6$, $[M + H]^+$, 472.1755; found 472.1754.

*1-(5-(2-Hydroxy-3,6,7-trimethoxyphenanthren-9-yl)-7,8-dihydro-[1,3]dioxolo[4,5-g]isoquinolin-6(5H)-yl)ethanone (**22t**).* White solid, 77 mg, yield: 91%. ^{1}H NMR (400 MHz, DMSO-d_6) δ 9.32 (s, 1H), 8.02 (s, 1H), 8.01 (s, 1H), 7.96 (s, 1H), 7.23 (s, 1H), 6.91 (s, 1H), 6.84 (s, 1H), 6.66 (s, 2H), 6.02 (s, 1H), 5.99 (s, 1H), 4.02 (s, 3H), 3.88 (s, 3H), 3.72–3.67 (m, 1H), 3.25–3.17 (m, 1H), 3.02–2.93 (m, 1H), 2.79–2.74 (m, 1H), 2.12 (s, 3H). ^{13}C NMR (100 MHz, DMSO-d_6) δ 169.32, 149.46, 149.31, 148.85, 146.95, 146.90, 146.07, 133.96, 129.18, 128.79, 127.07, 125.50, 125.29, 124.94, 123.71, 112.39, 108.97, 108.73, 106.42, 104.57, 104.24, 101.26, 56.46, 56.41, 56.09, 52.72, 39.28, 28.66, 21.70. HRMS calcd for $C_{29}H_{28}NO_7$, $[M + H]^+$, 502.1680; found 502.1682.

*1-(5-(3-Hydroxy-2-methoxyphenanthro[2,3-d][1,3]dioxol-6-yl)-7,8-dihydro-[1,3]dioxolo[4,5-g]isoquinolin-6(5H)-yl)ethanone (**22u**).* White solid, 78 mg, yield: 90%. ^{1}H NMR (400 MHz, DMSO-d_6) δ 9.37 (s, 1H), 8.28 (s, 1H), 8.00 (s, 1H), 7.96 (s, 1H), 7.13 (s, 1H), 6.91 (s, 1H), 6.84 (s, 1H), 6.70 (s, 1H), 6.62 (s, 1H), 6.18 (s, 1H), 6.15 (s, 1H), 6.01 (s, 1H), 5.98 (s, 1H), 4.00 (s, 3H), 3.70–3.68 (m, 1H), 3.27–3.21 (m, 1H), 3.01–2.98 (m, 1H), 2.80–2.76 (m, 1H), 2.27–2.24 (m, 1H), 2.12 (s, 3H). ^{13}C NMR (100 MHz, DMSO-d_6) δ 169.23, 149.58, 147.84, 147.18, 147.10, 146.89, 146.08, 134.30, 129.21, 128.72, 127.35, 126.97, 126.14, 125.49, 124.25, 112.06, 108.93, 108.64, 104.24, 102.94, 101.69 (×2), 101.25, 56.38, 52.79, 39.22, 28.56, 21.88. HRMS calcd for $C_{28}H_{23}NO_7Na$, $[M + Na]^+$, 508.1367; found 508.1377.

Biology

Kinase Glo® luminescent kinase assays. PAK4 was preincubated with PF-3758309 (**1**) and all the target molecules for 30 minutes, and then the kinase assay was performed. Reactions were stopped by the addition of an equal volume of Kinase-Glo reagent (Promega) and incubated for 10 min at room temperature. Chemiluminescence was measured at 555 nm (20 nm emission slit) using a Cary Eclipse fluorescence spectrophotometer (Tecan) equipped with a microplate carrier.

MTT assays. The human breast cell line MCF-7, the human pulmonary carcinoma cell line A-549 and the human fibrosarcoma cell line HT-1080 were cultured in RPMI-1640 medium containing 10% FBS, 100 U mL^{-1} streptomycin and 100 U mL^{-1} penicillin at 37 °C under a humidified atmosphere containing 5% CO_2.

The *in vitro* anti-proliferative activities of some of the target compounds were determined by the MTT (Sigma) assay. MCF-7, A549, and HT1080 (1×10^4 per well) were plated in 0.1 mL of the medium containing 10% FBS in 96-well Corning plates; 24 h later, the medium was removed and replaced with 0.1 mL medium containing the indicated concentrations of PF-3758309 and the target compounds for 24 h. At the end of the incubation, the capability of cellular proliferation was measured by the modified tetrazolium salt-3-(4,5-dimethylthiozol-2-yl)-2,5-biphenyl-tetrazolium bromide (MTT) assay. For this, 0.01 mL of MTT solution (5 mg mL^{-1} in PBS) was added to each well. After a 4 h incubation at 37 °C, the medium was replaced by 0.15 mL DMSO. After 15 min of incubation at 37 °C, the optical densities at 595 nm were measured using a Microplate Reader (BIO-RAD). The data were calculated and plotted as the percent viability compared to the control. The 50% inhibitory concentration (IC_{50}) was defined as the concentration that reduced the absorbance of the untreated wells by 50% of the vehicle in the MTT assay.

Cell-cycle analysis by flow cytometry. MCF-7 cells (8×10^4 cells) were incubated with the indicated concentrations of **21a** for the indicated time. After incubation, cells were collected, washed with PBS and then suspended in a staining buffer (10 μg mL^{-1} propidium iodide, 0.5% Tween-20, 0.1% RNase in PBS). The cells were analyzed using a FACSVantage flow cytometer with the Cell Quest acquisition and analysis software program (Becton Dickinson and Co., San Jose, CA). Gating was set to exclude cell debris, doublets and clumps.

Analysis of cell apoptosis. The ability of **21a** to induce cell apoptosis of A549 cells was quantified by annexin V and PI staining and flow cytometry, as described previously. Briefly, after treatment with **21a** for 24 h, cells were collected and washed with PBS twice, and subjected to annexin V and propidium iodide staining using an annexin-V FITC apoptosis kit following the step-by-step protocol provided by the manufacturer. After staining, flow cytometry was performed for the quantification of apoptotic cells.

Cell invasion assay. Matrigel invasion assays were performed using modified Boyden chambers with polycarbonate Nucleopore membrane. Precoated filters (6.5 mm in diameter, 8 μm pore size, and matrigel 100 μg cm^{-2}) were rehydrated with 100 μL medium. Then, 1×10^5 cells in 100 μL serum-free DMEM supplemented with 0.1% bovine serum albumin were placed in the upper part of each chamber, whereas the lower compartments were filled with 600 μL DMEM containing 10% serum. After incubating for 18 h at 37 °C, non-invaded cells were removed from the upper surface of the filter with a cotton swab, and the invaded cells on the lower surface of the filter were fixed, stained, photographed and counted under high-power magnification.

Lentiviral production and infection. Recombinant lentiviruses including PAK4-Lentivirus, PAK4-RNAi-Lentivirus and pGC FU-GFP-LV, NC-GFP-LV vectors were purchased from Shanghai GeneChem Company. To stably overexpress PAK4, cells were infected with lentivirus carrying PAK4, and then selected with puromycin (1.5 μg mL^{-1}). The pGC FU-GFP-LV vector was used as control.

Western blot analysis. To determine the expression of protein, whole cell extracts were prepared from 1×10^6 cells in RIPA lysis buffer (50 mM Tris/HCl pH 7.4, 150 mM NaCl, 1% Nonidet P-40, 0.25% Na-deoxycholate, 1 mM EDTA and protease inhibitor cocktail). Equal amounts of denatured protein were separated by SDS-PAGE and transferred to a PVDF membrane (Millipore). The membrane was blocked with 5% nonfat dry milk in TBS-T (20 mM Tris, pH 7.4, 137 mM NaCl, 0.05% Tween-20) for 3 h at room temperature, and the proteins were

probed with specific antibodies: CDK2, CDK4, CDK6, cyclin D1 (Neomarker), cyclin D3, cyclin B1, Bcl-2, BAX, caspase 3, caspase 8, LIMK1, phospho-LIMK1, cofilin, phospho-cofilin, PAK4, phospho-PAK4/Ser474, SCG-10, phospho-SCG10/Ser50. All PVDF membranes were detected by chemiluminescence (ECL, Pierce Technology). To ensure equal loading, membranes were stripped and reprobed with antibody against GAPDH and MMP2 (Shang Hai Kangchen).

Conclusions

Following the identification of (−)-β-hydrastine as a PAK4 inhibitor from our in-house natural product database, we undertook a detailed SAR investigation aimed at improving potency as well as increasing metabolic stability of this compound. A combination of traditional and modern medicinal chemistry principles led to the identification of a novel, potent, ATP-competitive PAK4 inhibitor (**21a**), which demonstrated target modulation in PAK4 driven cancer cells (MCF-7). It was shown that compound **21a** suppressed the expression of cyclin D (cyclin D1, D3) and CDKs (CDK2, 4, 6), in turn inhibiting the transition of cells from the G1 phase to S phase, and resulted in the anti-proliferative effect on MCF-7 cells together with the induction of apoptosis. Furthermore, Transwell and Western blot studies suggested that compound **21a** caused significant inhibition of migration and invasion in breast cancer cells *via* blockage of the PAK4/LIMK1/cofilin, PAK4/MMP2, or PAK4/SCG10 signaling pathways. The molecular docking study demonstrated possible novel binding modes for the interactions between compound **21a** and PAK4. In summary, this work not only broadened the scope of searching for PAK4 kinase inhibitors with novel scaffolds, but also laid a solid foundation for looking for more potent PAK4 inhibitors in the future.

Acknowledgements

We gratefully acknowledge the financial support from the National Natural Science Foundation of China (grant 1230077, 81102379, 81001092, and J1210029), the National High Technology Research and Development Program of China (grant 2007AA02Z305) and Program for Innovative Research Team of the Ministry of Education, and Program for Liaoning Innovative Research Team in University.

Notes and references

1 E. Manser, T. Leung, H. Salihuddin, Z. S. Zhao and L. Lim, *Nature*, 1994, **367**, 40–46.
2 R. H. Daniels and G. M. Bokoch, *Trends Biochem. Sci.*, 1999, **9**, 350–355.
3 H. Maruta and E. D. Korn, *J. Biol. Chem.*, 1977, **23**, 8329–8332.
4 C. M. Wells and G. E. Jones, *Biochem. J.*, 2010, **425**, 465–473.
5 G. M. Bokoch, *Annu. Rev. Biochem.*, 2003, **1**, 743–781.
6 L. E. Arias-Romero and J. Chernoff, *Biol. Cell*, 2008, **2**, 97–108.
7 M. Lei and W. Lu, *Cell*, 2000, **3**, 387–397.
8 Y. Baskaran, Y. W. Ng, W. Selamat, F. T. P. Ling and E. Manser, *EMBO Rep.*, 2012, **7**, 653–659.
9 F. M. Vega and A. J. Ridley, *FEBS Lett.*, 2008, **14**, 2093–2101.
10 J. Zhang, J. Wang, Q. Guo, Y. Wang, Y. Zhou, H. Peng, M. S. Cheng, D. M. Zhao and F. Li, *Cancer Lett.*, 2012, **1**, 24–32.
11 A. E. Dart and C. M. Wells, *Eur. J. Cell Biol.*, 2013, **4**, 129–138.
12 S. Chen, T. Auletta, O. Dovirak, C. Hutter, K. Kuntz, J. Kendall, H. Han, D. D. Von Hoff, R. Ashfaq, A. Maitra, C. A. Iacobuzio-Donahue, R. H. Hruban and R. Lucito, *Cancer Biol. Ther.*, 2008, **11**, 1793–1802.
13 M. G. Callow, F. Clairvoyant, S. Zhu, B. Schryver, D. B. Whyte, J. R. Bischoff, B. Jallal and T. Smeal, *J. Biol. Chem.*, 2001, **1**, 550–558.
14 A. Tasneem, S. Kerry, R. W. M. John, E. J. Gareth and M. W. Claire, *Cell. Signal.*, 2008, **7**, 1320–1328.
15 M. K. Y. Siu, H. Y. Chan, D. S. H. Kong, E. S. Y. Wong, O. G. W. Wong, H. Y. S. Ngan, K. F. Tam, H. Zhang, Z. Li, Q. K. Y. Chan, S. W. Tsao, S. Stromblad and A. N. Y. Cheung, *Proc. Natl. Acad. Sci. U. S. A.*, 2010, **43**, 18622–18627.
16 V. Delorme, M. Machacek, C. DerMardirossian, K. L. Anderson, T. Wittmann, D. Hanein, S. C. Waterman, G. Danuser and G. M. Bokoch, *Dev. Cell*, 2007, **5**, 646–662.
17 X. Li, Q. Ke, Y. Li, F. Liu, G. Zhu and F. Li, *Int. J. Biochem. Cell Biol.*, 2010, **1**, 70–79.
18 C. Dan, A. Kelly, O. Bernard and A. Minden, *J. Biol. Chem.*, 2001, **34**, 32115–32121.
19 P. X. Chen, M. J. Zeng, Y. Zhao and X. L. Fang, *Oncol. Rep.*, 2014, **5**, 2070–2076.
20 Y. Liu, H. Xiao, Y. Tian, T. Nekrasova, X. Hao, H. J. Lee, N. Suh, C. S. Yang and A. Minden, *Mol. Cancer Res.*, 2008, **6**, 215–224.
21 R. Kumar, A. E. Gururaj and C. J. Barnes, *Nat. Rev. Cancer*, 2006, **6**, 459–471.
22 P. R. Molli, D. Q. Li, B. W. Murray, S. K. Rayala and R. Kumar, *Oncogene*, 2009, **28**, 2545–2555.
23 C. X. Guo, I. McAlpine, J. H. Zhang, D. D. Knighton, S. Kephart, M. C. Johnson, H. Li, D. Bouzida, A. Yang and L. Dong, *J. Med. Chem.*, 2012, **10**, 4728–4739.
24 (*a*) B. W. Murray, C. Guo, J. Piraino, J. K. Westwick, C. Zhang, J. Lamerdin, E. Dagostino, D. Knighton, C. M. Loi, M. Zager, E. Kraynov, I. Popoff, J. G. Christensen, R. Martinez, S. E. Kephart, J. Marakovits, S. Karlicek, S. Bergqvist and T. Smeal, *Proc. Natl. Acad. Sci. U. S. A.*, 2010, **20**, 9446–9451; (*b*) J. R. Byung, L. Hyuk, K. Seong-Ho, H. N. Jung, C. W. Sik, Y. T. Jeong, L. Jeongmin, L. S. Jong, Y. C. Jae, H. K. Seong and Y. L. Sang, *Mol. Cell. Biochem.*, 2014, **1–2**, 69–77.

25 L. S. Rosen, T. A. Blumenkopf, A. Breazna, S. Darang, J. D. Gallo, J. Goldman, D. Wang, L. Mileshkin and S. G. Eckhardt, *Mol. Cancer Ther.*, 2011, **11**(Suppl.), Abstract A177.
26 B. J. Ryu, S. Kim, B. Min, K. Y. Kim, J. S. Lee, W. J. Park, H. Lee, S. H. Kim and S. Y. Park, *Cancer Lett.*, 2014, **1**, 45–50.
27 S. T. Staben, J. A. Feng, K. Lyle, M. Belvin, J. Boggs, J. D. Burch, C. C. Chua, H. Cui, A. G. DiPasquale, L. S. Friedman, C. Heise, H. Koeppen, A. Kotey, R. Mintzer, A. Oh, D. A. Roberts, L. Rouge, J. Rudolph, C. Tam, W. Wang, Y. Xiao, A. Young, Y. Zhang and K. P. Hoeflich, *J. Med. Chem.*, 2014, **3**, 1033–1045.
28 B. C. Nadja, A. J. Hiyas, W. A. Laynez, S. K. Jeffrey and R. H. Alexander, *Planta Med.*, 2012, **14**, 1556–1561.
29 S. Y. Yin, Y. M. Kim, J. J. Lee, C. M. Jin, Y. J. Yang, S. K. Park, S. K. Yoo and M. K. Lee, *Biol. Pharm. Bull.*, 2007, **8**, 1547–1550.
30 (*a*) B. Sung, K. S. Ahn and B. B. Aggarwal, *Cancer Res.*, 2010, **8**, 3259–3268; (*b*) N. Jhaveri, H. Cho, S. Torres, W. Wang, A. H. Schönthal, N. A. Petasis, G. L. Stan, M. H. Florence and T. C. Chen, *Cancer Lett.*, 2011, **2**, 245–252.
31 S. Yamashita, N. Kurono, H. Senboku, M. Tokuda and K. Orito, *Eur. J. Org. Chem.*, 2009, 1173–1180.
32 C. R. Su, A. G. Damu, P. C. Chiang, K. F. Bastow, N. Morris, L. Susan, K. H. Lee and T. S. Wu, *Bioorg. Med. Chem.*, 2008, **11**, 6233–6241.
33 S. D. Jones, J. W. Liebeschuetz, P. J. Morgan, C. W. Murray, A. D. Rimmer, J. M. E. Roscoe, B. Waszkowycz, P. M. Welsh, W. A. Wylie and S. C. Young, *Bioorg. Med. Chem. Lett.*, 2001, **5**, 733–736.
34 M. Lafrance, N. Blaquiere and K. Fagnou, *Eur. J. Org. Chem.*, 2007, 811–825.
35 R. J. Li, J. Wang, Z. Xu, W. X. Huang, J. Li, S. F. Jin, D. M. Zhao and M. S. Cheng, *ChemMedChem*, 2014, **5**, 1012–1022.
36 J. J. L. Liao, *J. Med. Chem.*, 2007, **3**, 409–424.
37 M. J. McGregor, *J. Chem. Inf. Model.*, 2007, **6**, 2374–2382.

